

Supplementary Information

SI Material and Methods.

Taxon and Locus Sampling. Families were sampled proportionally to their species richness. The Teloschistaceae included 97 species (including potentially new species) and 9 genera. The family Megalosporaceae was represented by five species and 3 genera, and the tropical families Brigantiaeaceae and Letrouitiaceae, by three species each. This sampling represents about 15% of species currently accepted within the Teloschistales and covers most phenotypic diversity within the group. Of the 511 sequences included in this study, 270 were generated anew and 241 were retrieved from GenBank or the WASABI database of AFToL (1) (see Table S3 for voucher and GenBank accession numbers information). DNA extraction, amplification, and sequencing followed (2).

Alignments and Datasets. Newly generated sequence fragments were subjected to BLAST searches for a first verification of their identities. They were assembled and edited using DNASTAR Lasergene Core Suite 11 (DNASTAR Inc., Madison, WI), and aligned manually with Mesquite 2.75 (3). The nuclear ribosomal loci were aligned with the help of the secondary structure as described in (2). Ambiguously aligned regions (*sensu* (4)) and introns were delimited manually and excluded from subsequent analyses. At least three of the six targeted loci were available for all taxa included in this study. The concatenated alignment was deposited in TreeBASE (accession number 18015).

Phylogenetic Analyses.

Detecting conflict: No incongruency was detected among the six loci used in our analyses. Of particular relevance to this study, no incongruence was observed in shorter internodes located deeper in the phylogeny. A conflict was assumed to be significant if two different relationships (one being monophyletic and the other being non-monophyletic) for the same set of taxa were both supported with bootstrap values $\geq 70\%$ (5). Based on this approach, we initially detected significant conflicts only for a few internodes, and further examination revealed that these were due to misidentification or contamination. When the corresponding five sequences were removed from the dataset, we detected no significant conflict among single-locus trees. We then concatenated the individual alignments to form one conflict-free dataset.

Bayesian and maximum likelihood analyses: In the Bayesian analyses, the AIC in MrModeltest 2.3 (6) was used to choose the model of molecular evolution. Prior distributions were as in (2). Two analyses of four chains were run for 50 M using MrBayes 3.2.2 (7), with trees sampled every 500 generations. Log-likelihood scores were plotted against generation time with Tracer v1.6 ((8); <http://beast.bio.ed.ac.uk/Tracer>) and assigned stationarity when they reached a stable equilibrium

value (9), when the average standard deviation of split frequencies (ASDSF) across runs dropped below 0.01, and the potential scale reduction factor (PSRF) of the parameters and branch lengths was equal or close to 1. This was also verified with the AWTY program, <http://ceb.csit.fsu.edu/awty>, (10). A burn-in sample of 30,000 trees was discarded for each run. The remaining 140,000 trees were used to estimate branch lengths and posterior probabilities.

Maximum likelihood analysis was computed in RAxML with the same partitions as in Bayes (Table S4) but with *RPB1* and *RPB2* 1st and 2nd codons unlinked, a GTRGAMMA model of nucleotide substitution, and 1,000 replicates.

Classification of the Teloschistaceae: As discussed in the main text, the taxonomy of this group of lichens, especially the family Teloschistaceae, has been habitually highly controversial. In the last years, several alternative classifications have been proposed including new and resurrected genera (e.g., (11, 12)). Regardless of exceptional efforts to cover a broad taxon sampling in some of these studies (e.g., (11)), they have (a) relied on only one to three ribosomal RNA-coding genes, (b) failed to find strong support for several of the newly delimited genera as monophyletic, and (c) disagreed over many generic circumscriptions, showing a lack of consistency. Although the present 6-gene phylogeny brings significant levels of support for a number of clades, a complete reassessment including phenotypic information and a thorough revision of all current available names are urgently needed to procure a more secure and stable nomenclature at the generic level. While we plan to address this complex issue in a forthcoming study, on the grounds of simplicity and practicality we have used here the traditional generic names for the group, recently included in a ‘without-prejudice’ list of generic names of fungi for protection under the International Code of Nomenclature (13), being aware that their current circumscription is polyphyletic in some cases.

Dating Analyses. Settings for the two analyses used in this study are described below.

Eukaryotes dataset: A five-gene dataset (*RPB1*, *RPB2*, *EF1a*, nrLSU, and nrSSU) was assembled to comprise 8,324 characters and 114 taxa, including 13 species of Teloschistales and 101 taxa representing all main groups of fungi as well as several plants, animals, and protists. We used a Bayesian approach to estimate divergence times as implemented in the software package BEAST v.1.7.4. Input files were prepared using BEAUti (14). A randomly generated starting tree was used, but several nodes were constrained as monophyletic (see Table S5) based on previous results (15). The nucleotide substitution model was set to GTR + Gamma + Invariant sites, with simultaneously estimated base frequencies, four gamma categories, and five gene partitions as well as partitions for the three codon positions of *RPB1*, *RPB2*, and *EF1a*. For the clock, we used an uncorrelated log normal model, with simultaneously estimated rates. We used a Yule tree prior, which assumes a constant speciation rate per lineage. Calibrations were set as prior distributions as described in (15), with few minor modifications (Table S6). The analysis was run for 40 M

generations and parameters were sampled every 1,000 generations. The software Tracer v.1.6 was used to analyze the trace files (8). Trees were annotated using TreeAnnotator v.1.7.5 with a burnin of 10,000 trees (14) and visualized in FigTree v.1.4.2 (<http://tree.bio.ed.ac.uk/software/figtree>; Fig. S6).

Teloschistales dataset: A six-locus dataset [*RPB1*, *RPB2* (two amplicons), 5.8S, mtSSU, and nrLSU] was assembled to obtain a chronogram (Fig. S1). This dataset included 4,643 characters and 108 taxa belonging to Teloschistales. The dataset was partitioned into five gene regions as well as three codon positions for both *RPB1* and *RPB2*. The nucleotide substitution model was the same as in the eukaryotes dataset. We used an uncorrelated log normal model for the clock and a Yule tree prior for the speciation rate per lineage. Calibrations were set as priors using normal distributions. The nine deepest nodes (node A-I; Figs. S1, S6) were calibrated as described in Table S7. Analysis were run and examined as for the eukaryotes dataset. Resulting age estimates for selected nodes are shown in Table S8.

Testing for Shifts in Diversification Rates. We performed multiple BAMM runs with four chains on the Teloschistales maximum clade credibility tree (MCCT), with 10 M generations of Markov Chain Monte Carlo (MCMC) sampling per run and evolutionary parameters sampled every 10,000 generations. We assessed convergence of BAMM runs by computing effective sample sizes of log-likelihoods, numbers of shifts, and evolutionary rate parameters using the CODA library in R; all parameters had effective sample sizes > 500. We reconstructed marginal distributions of net diversification rates for each branch in the MCC Teloschistales phylogeny using the posterior distribution of evolutionary parameters sampled using the rjMCMC algorithm in BAMM. We simulated prior shifts in order to compute Bayes Factors. We set a conservative prior of 1 for rate shifts under the compound Poisson process (poissonRatePrior), and constrained the location of possible rate-change events to occur only on branches with at least 10 descendant tips. We implemented the ‘time-flip’ proposal (time-constant and time-variable shifts) to avoid potential biased inference on speciation in some areas of the parameter space; rate shifts will lead to a constant-rate diversification process (MEDUSA-like) unless the data contains sufficient evidence for temporally varying macroevolutionary rate dynamics. According to the authors this model improves BAMM performance (see <http://bamm-project.org/time-flip.html>).

Ancestral Character State Estimations. The settings used in the different methods implemented in the ancestral character state estimation of binary traits were the following: 1) a Bayesian approach with BayesTraits (<http://www.evolution.reading.ac.uk/BayesTraits.html>) across a random subset of 500 post-burnin dated trees from the BEAST output. The Multistate Markov model was implemented to determine probabilities of character state change on each branch. Analyses were run for 10 M MCMC iterations, with 5 M as a burnin and trees sampled every 1,000

generations. Runs were carried out at least twice in order to check for convergence. In addition, we compared performance among three sets of analyses implementing a reversible-jump (RJ) MCMC on an unconstrained model, an unconstrained model without RJ, and a constrained model with forward (q_{01}) and backward (q_{10}) transition rates set to equal, without RJ. In all implementations we used hyper priors for discrete rate parameters. We tested for different intervals (0 0.01 to 0 100) with hyper exponential and hyper gamma priors on all parameters. Harmonic means (HMEs) and Bayes Factors (BFs) were compared between analyses. Best-fit models were selected on the basis of $BF > 2$. Reconstructions were implemented with a MRCA approach. In all traits, BayesTraits supported a constrained model over a Reverse jump and a hyper prior unconstrained, with transition rates set to equal and a hyper exponential prior on all parameters drawn from a uniform with different ranges depending on the trait (Table S9). These analyses accounted for phylogenetic uncertainty. 2) A maximum likelihood approach with BiSSE (16); implemented in diversitree 0.9-2 package (17), using marginal reconstructions and the model selected in the diversification analyses described in the main text. After assessing several sampling regimes in BiSSE, we estimated the reconstructions for a 10% taxon sampling as the most realistic scenario in all traits. 3) A maximum likelihood approach with the *corHMM* function contained within the R package *corHMM* (18, 19), using marginal reconstructions, considering a ‘*hidden rates model*’ (HRM), and testing for different numbers of hidden rate classes for the evolution of traits. Several random starts were performed, different initial values used for the likelihood search ($ip = 0.001$ to 1), and root was set to ‘maddfitz’ to implement the same procedure as in (16) and (20). Model fit was assessed by comparing AICc values. A 2-rate model of phenotypical evolution clearly outperformed a 1-rate model only for the shade character (Table S10). We used *corHMM* under a 1-rate model as a simple maximum likelihood reconstruction.

Testing for State-Dependent Diversification Rates. We implemented a full 10-parameter BiSSE-ness model (21), a 9-parameter model where the probability of character change at speciation is $p_{0c} = 0$, an 8-parameter model where $p_{0c} = p_{1c}$, an 8-parameter with speciation and extinction rates constrained to equal independently of the state, and a 6-parameter model with one speciation and extinction rates and $p_{0c} = p_{1c}$. We used AIC scores to compare these models and we examined all BiSSE and BiSSE-ness models with different taxon sampling scenarios, with assumptions that we had sampled from 10% up to 90% of the taxa within the Teloschistaceae.

1. Miadlikowska J, et al. (2014) A multigene phylogenetic synthesis for the class Lecanoromycetes (Ascomycota): 1307 fungi representing 1139 infrageneric taxa, 317 genera and 66 families. *Mol Phylogenet Evol* 79C:132–168.
2. Gaya E, et al. (2012) Implementing a cumulative supermatrix approach for a comprehensive

phylogenetic study of the Teloschistales (Pezizomycotina, Ascomycota). *Mol Phylogenet Evol* 63(2):374–387.

3. Maddison WP, Maddison DR (2011) Mesquite: A modular system for evolutionary analysis. Version 2.75(<http://mesquiteproject.org>).
4. Lutzoni F, Wagner P, Reeb V, Zoller S (2000) Integrating ambiguously aligned regions of DNA sequences in phylogenetic analyses without violating positional homology. *Syst Biol* 49(4):628–651.
5. Mason-Gamer RJ, Kellogg EA (1996) Testing for phylogenetic conflict among molecular data sets in the tribe Triticeae (Gramineae). *Syst Biol* 45(4):524–545.
6. Nylander JAA, Ronquist F, Huelsenbeck JP, Nieves-Aldrey J (2004) Bayesian phylogenetic analysis of combined data. *Syst Biol* 53(1):47–67.
7. Ronquist F, et al. (2012) MrBayes 3.2: Efficient Bayesian phylogenetic inference and model choice across a large model space. *Syst Biol* 61(3):539–542.
8. Rambaut, A, Suchard M, Xie D, Drummond AJ (2014) Tracer v. 1.6. Available at: <http://beast.bio.ed.ac.uk/Tracer>.
9. Huelsenbeck JP, Ronquist F (2001) MrBayes: Bayesian inference of phylogenetic trees. *Bioinformatics* 17(8):754–755.
10. Nylander JAA, Wilgenbusch JC, Warren DL, Swofford DL (2008) AWTY (are we there yet?): A system for graphical exploration of MCMC convergence in Bayesian phylogenetics. *Bioinformatics* 24(4):581–583.
11. Arup U, Söchting U, Frödén P (2013) A new taxonomy of the family Teloschistaceae. *Nordic J Bot* 31(1):016–083.
12. Kondratyuk SY, Kärnefelt I, Thell A, Elix JA (2014) A revised taxonomy for the subfamily Caloplacoideae (Teloschistaceae, Ascomycota) based on molecular phylogeny. *Acta Bot Hung* 56(1-2):93–123.
13. Kirk PM, et al. (2013) A without-prejudice list of generic names of fungi for protection under the International Code of Nomenclature for algae, fungi, and plants. *IMA Fungus* 4(2):381–443.
14. Drummond AJ, Rambaut A (2007) BEAST: Bayesian evolutionary analysis by sampling trees. *BMC Evolutionary Biology* 7(1):214.
15. Gueidan C, Ruibal C, de Hoog GS, Schneider H (2011) Rock-inhabiting fungi originated during periods of dry climate in the late Devonian and middle Triassic. *Fungal Biol* 115(10):987–996.
16. Maddison W, Midford P, Otto S (2007) Estimating a binary character's effect on speciation

and extinction. *Syst Biol* 56(5):701–710.

17. FitzJohn RG (2012) Diversitree: comparative phylogenetic analyses of diversification in R. *Methods Ecol Evol* 3(6):1084–1092.
18. Beaulieu JM, O'Meara BC, Donoghue MJ (2013) Identifying hidden rate changes in the evolution of a binary morphological character: the evolution of plant habit in campanulid angiosperms. *Syst Biol* 62(5):725–737.
19. Beaulieu JM, Donoghue MJ (2013) Fruit evolution and diversification in campanulid angiosperms. *Evolution* 67(11):3132–3144.
20. FitzJohn RG, Maddison WP, Otto SP (2009) Estimating trait-dependent speciation and extinction rates from incompletely resolved phylogenies. *Syst Biol* 58(6):595–611.
21. Magnuson-Ford K, Otto SP (2012) Linking the investigations of character evolution and species diversification. *Am Nat* 180(2):225–245.
22. Redecker D, Kodner R, Graham LE (2000) Glomalean fungi from the Ordovician. *Science* 289(5486):1920–1921.
23. Taylor TN, Remy W, Hass H (1994) Allomyces in the Devonian. *Nature* 367(6464):601.
24. Hibbett D, Grimaldi D, Donoghue M (1997) Fossil mushrooms from Miocene and Cretaceous ambers and the evolution of Homobasidiomycetes. *Am J Bot* 84(7):981.
25. Taylor TN, Hass H, Kerp H (1999) The oldest fossil ascomycetes. *Nature* 399(6737):648.
26. Rikkinen J, Poinar GO (2002) Fossilised *Anzia* (Lecanorales, lichen-forming Ascomycota) from European Tertiary amber. *Mycol Res* 106(08):984–990.
27. Schmidt AR, et al. (2010) Cretaceous African life captured in amber. *Proc Natl Acad Sci USA* 107(16):7329–7334.
28. Crane PR, Friis EM, Pedersen KR (1995) The origin and early diversification of angiosperms. *Nature* 374:27–33.
29. Douzery EJP, Snell EA, Baptiste E, Delsuc F, Philippe H (2004) The timing of eukaryotic evolution: does a relaxed molecular clock reconcile proteins and fossils? *Proc Natl Acad Sci USA* 101(43):15386–15391.

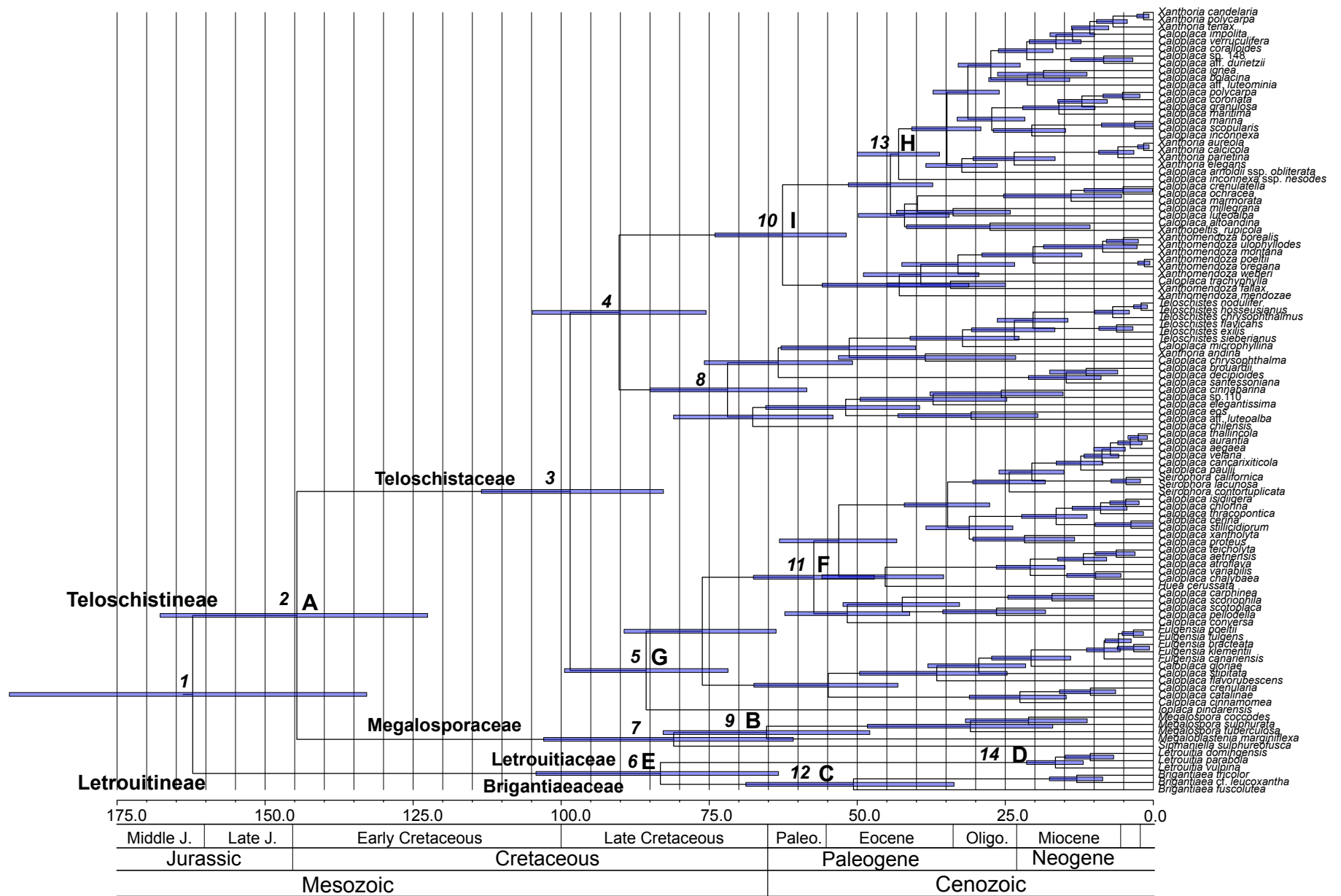


Fig. S1. Chronogram picturing divergence time estimates for 108 taxa of the order Teloschistales obtained using a six-locus dataset (*RPB1*, *RPB2* – two amplicons, 5.8S, mtSSU, and nrLSU). Bars correspond to 95% confidence intervals. The nine nodes marked with letters A-I correspond to the secondary calibrations obtained from the eukaryotes analyses (Fig. S6) as described in Table S7. Means and confidence interval values for nodes labeled 1-14 are shown in Table S8.

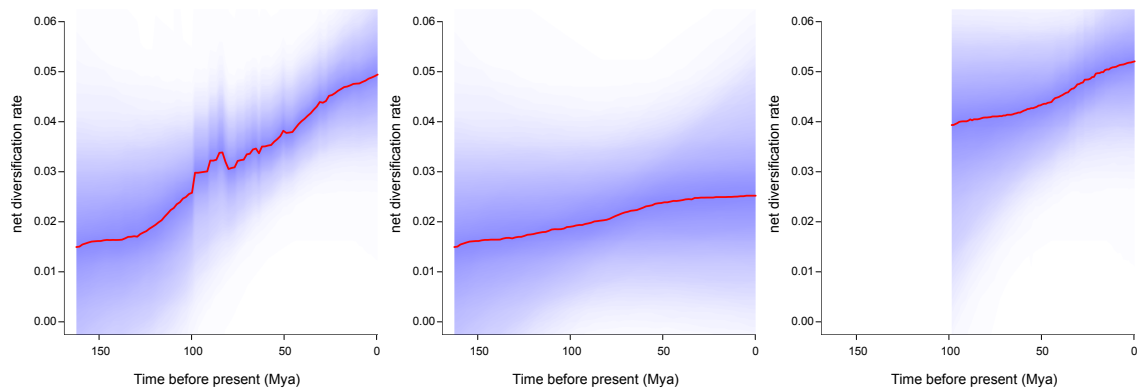


Fig. S2. Temporal dynamics in net diversification rates computed from the joint posterior density of macroevolutionary rate parameters simulated using the reversible jump MCMC algorithm in BAMM. Left graph shows overall mean rates through time for the Teloschistales (red line), with blue color density shading denoting confidence on evolutionary rate reconstructions at any point in time (10% through 90% Bayesian credible regions on the distribution of rates through time). Middle graph shows the rate-through-time estimates for the tropical Letrouitineae and Megalosporaceae alone. Right-hand graph shows the rate for the Teloschistaceae alone.

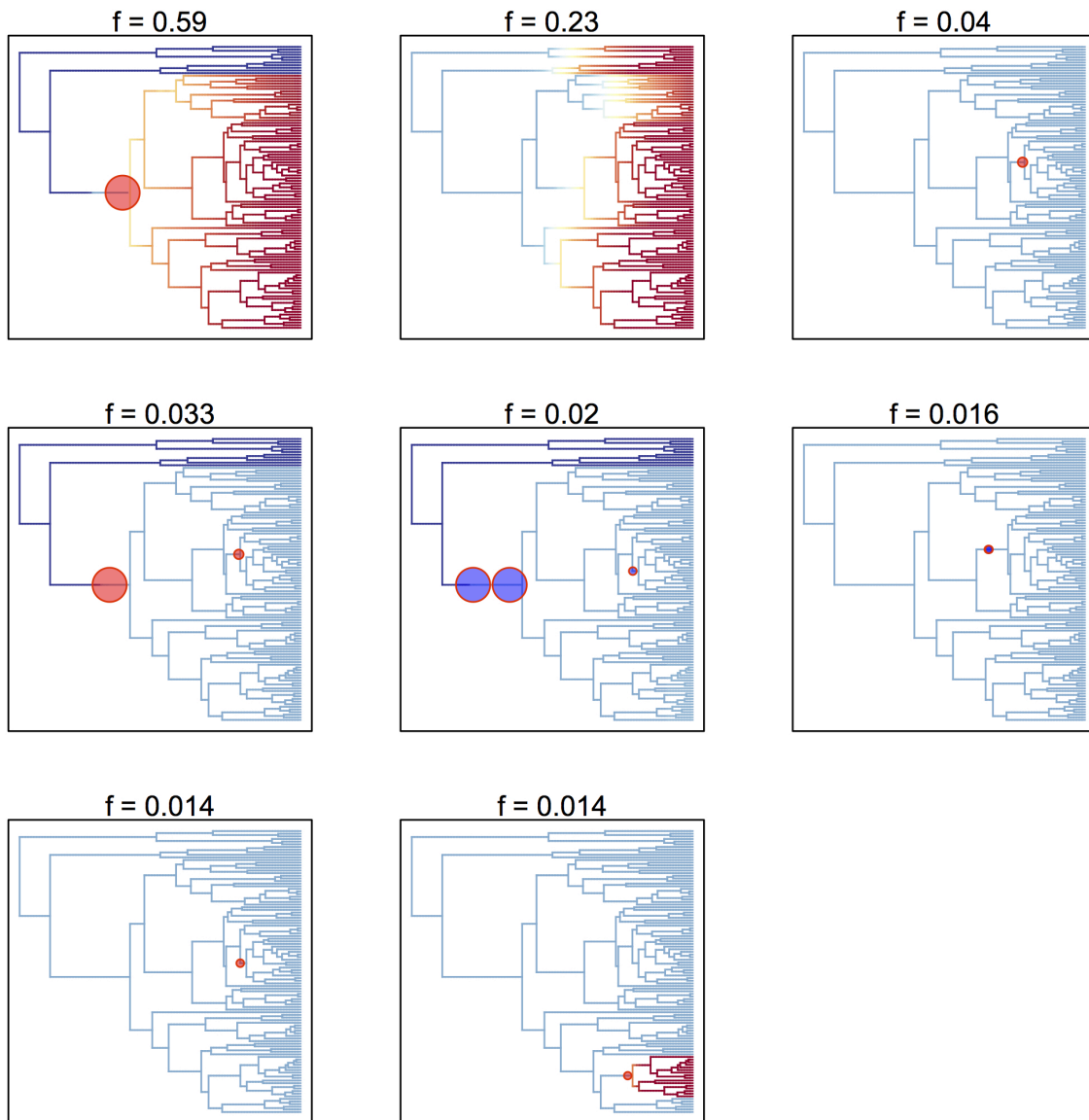


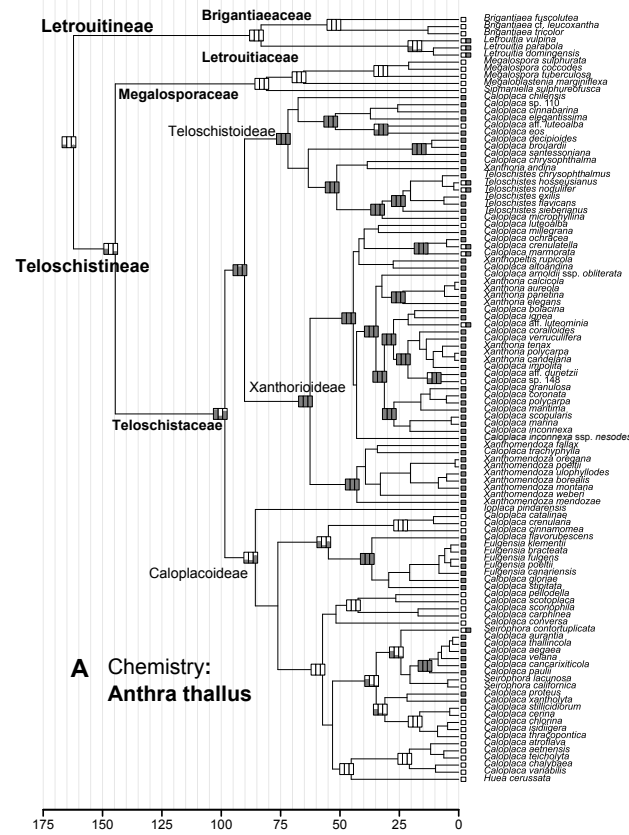
Fig. S3. Set of the most frequently sampled distinct shift configurations with the highest posterior probability. For each distinct shift configuration, the locations of rate shifts are shown as red (rate increases) and blue (rate decreases) circles, with circle size proportional to the marginal probability of the shift. Text labels (e.g., $f = 0.59$) denote the posterior probability of each shift configuration.

BayesTraits
BISSSE
corHMM 2-rates
corHMM 1-rate

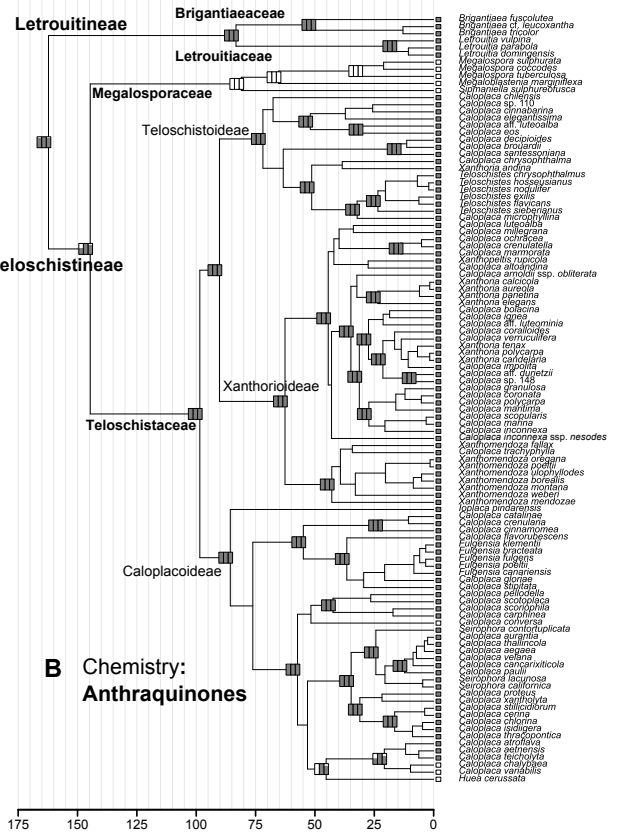
BayesTraits
BISSSE
corHMM 1-rate

BayesTraits
BISSSE
corHMM 1-rate

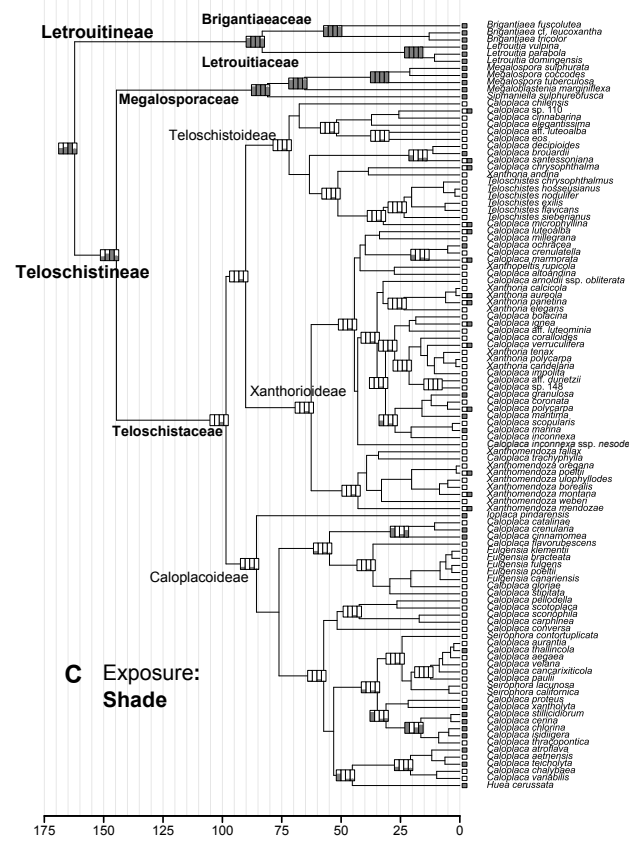
Present
Absent



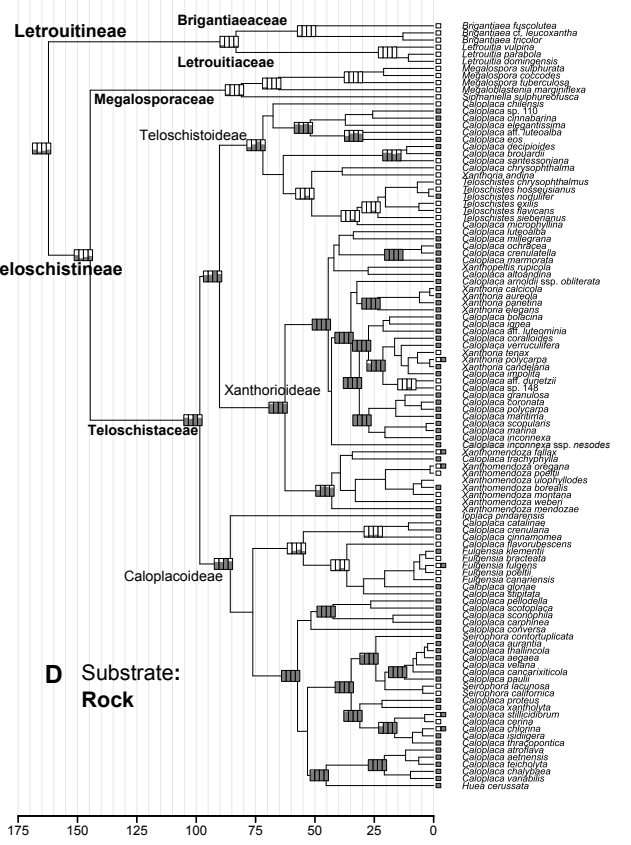
A Chemistry: Anthra thallus



B Chemistry: Anthraquinones



C Exposure: Shade



D Substrate: Rock

Fig. S4. (See next page for caption).

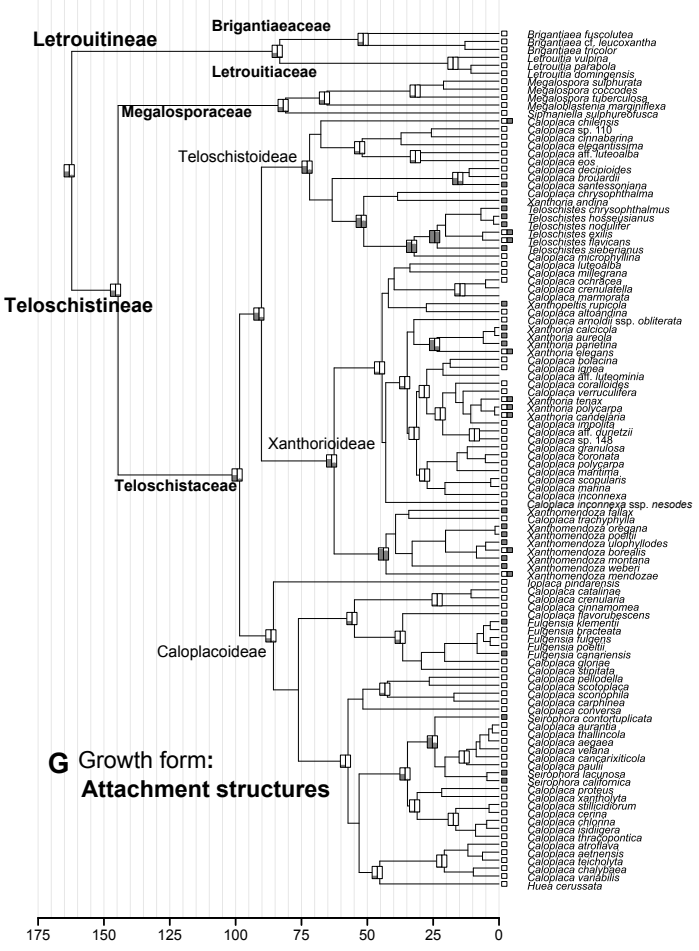
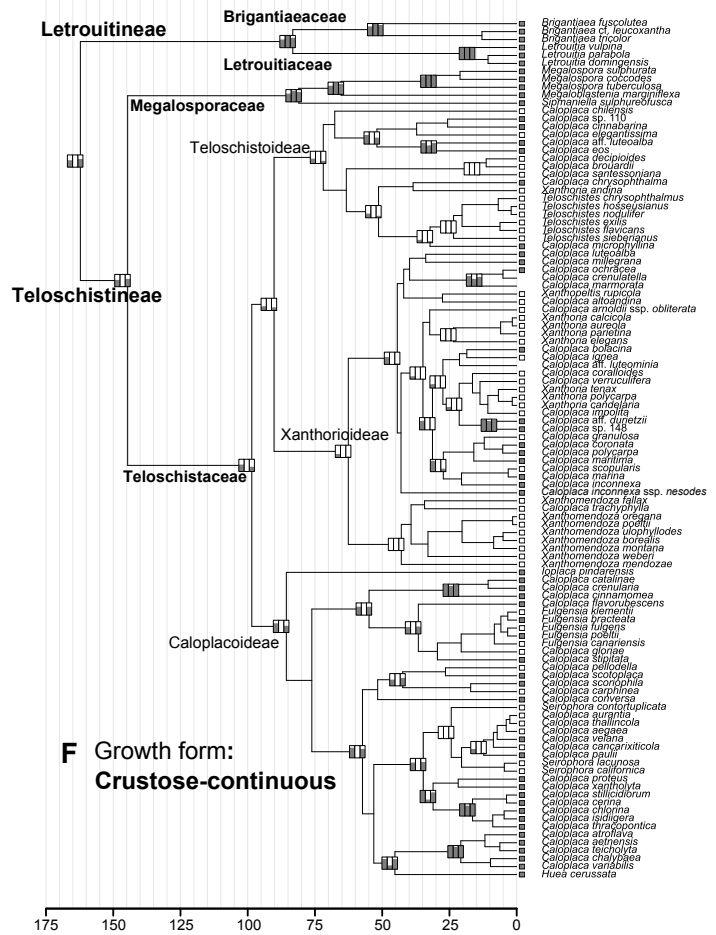
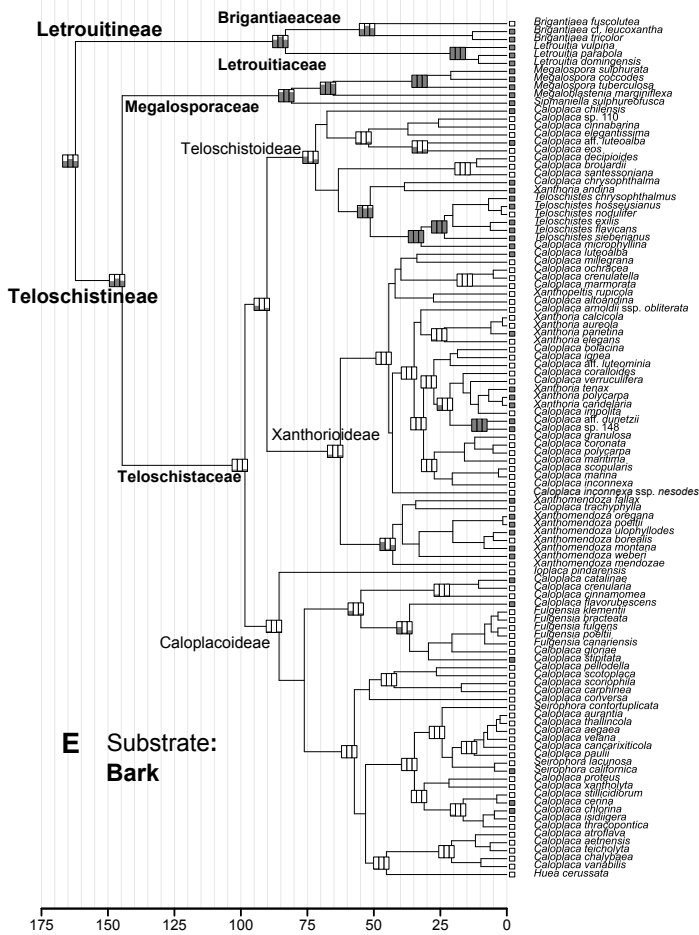


Fig. S4. Ancestral character state estimations for selected binary characters A) presence of anthraquinones in the thallus, B) presence of anthraquinones, C) shade exposure, D) rock substrate, E) bark substrate, F) crustose-continuous growth habit, G) attachment structures, using four different methods: (1) BayesTraits (accounting for model parameter and phylogenetic uncertainty); (2) BISSE [Binary State Speciation and Extinction; accounting for effects of trait evolution on species diversification among lineages; (16)], assuming that our phylogeny represents a random sample of extant species (20); (3) hidden rates model (HRM) implemented in R package *corHMM* (accounting for different rates of evolution in a binary character along different branches of a phylogeny, (18)); (4) standard maximum likelihood (ML) estimation. Boxes on internodes show the estimated probabilities of the trait being present (black) or absent (white). In figures with four boxes per internode, these represent (from left to right): BayesTraits, BiSSE, *corHMM* (2-rates) and *corHMM* (1-rate; equivalent to a standard ML ancestral state estimation) analyses. In figures with three boxes, *corHMM* (2-rates) is omitted due to lack of evidence for more than one evolutionary rate. In figures with two boxes, *corHMM* (2-rates) as well as BISSE analyses are omitted due to lack of evidence for trait correlation with diversification rates in the latter analysis.

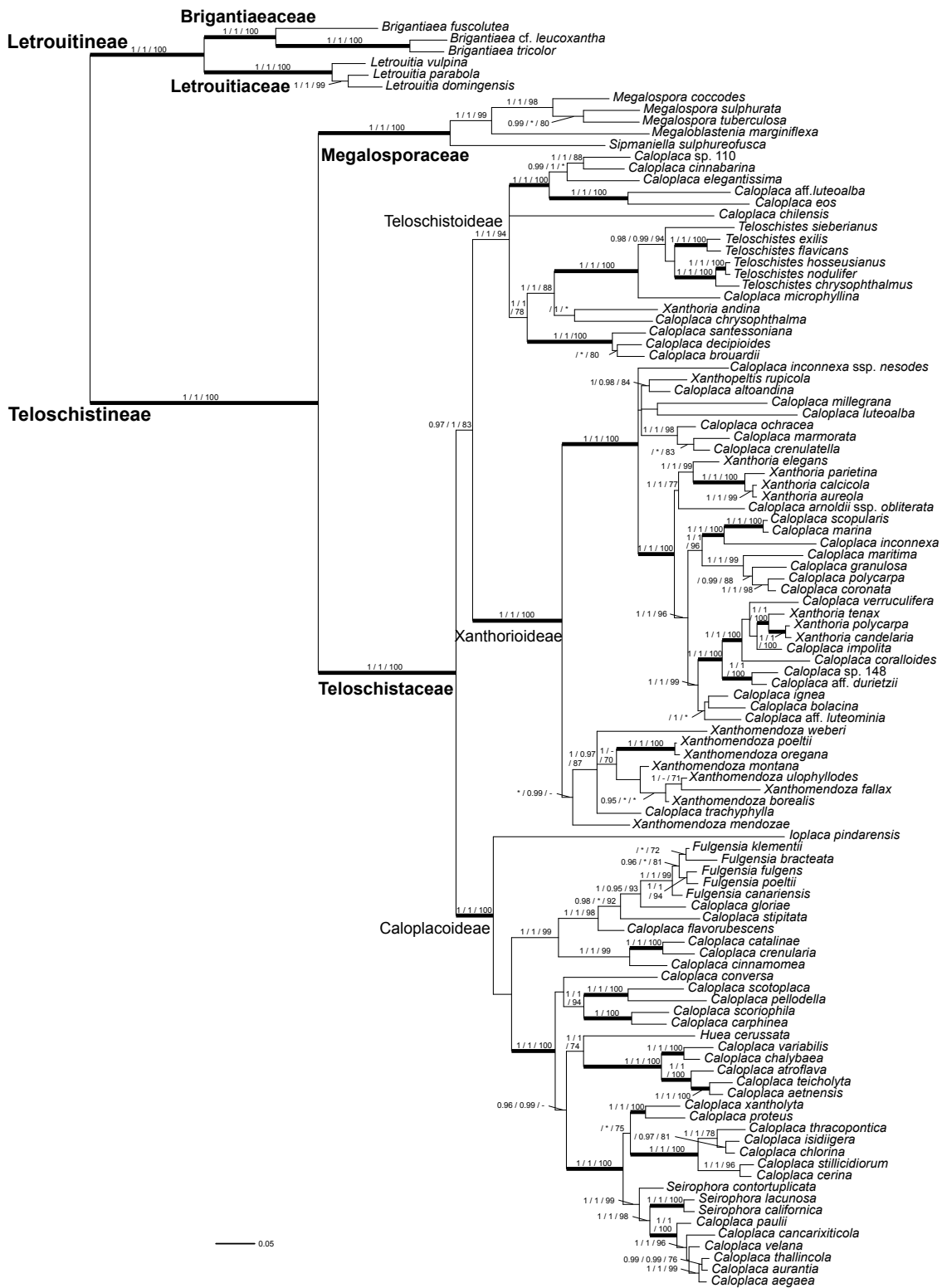


Fig. S5. Teloschistales phylogeny. Topology derived from Bayesian analysis performed on a combined 5.8S, nrLSU, mtSSU, *RPB1* and *RPB2* (two loci) supermatrix for 108 taxa. Only taxa with at least three genes were included. The suborder Letrouitineae was used to root the tree. The three support values associated with branches are Bayesian posterior probabilities from MrBayes / from BEAST / maximum likelihood bootstrap values from RAxML. Only bootstrap values $\geq 70\%$ or posterior probabilities ≥ 0.95 are indicated. Thickened branches denote posterior probabilities = 1.00 and bootstrap support values = 100.

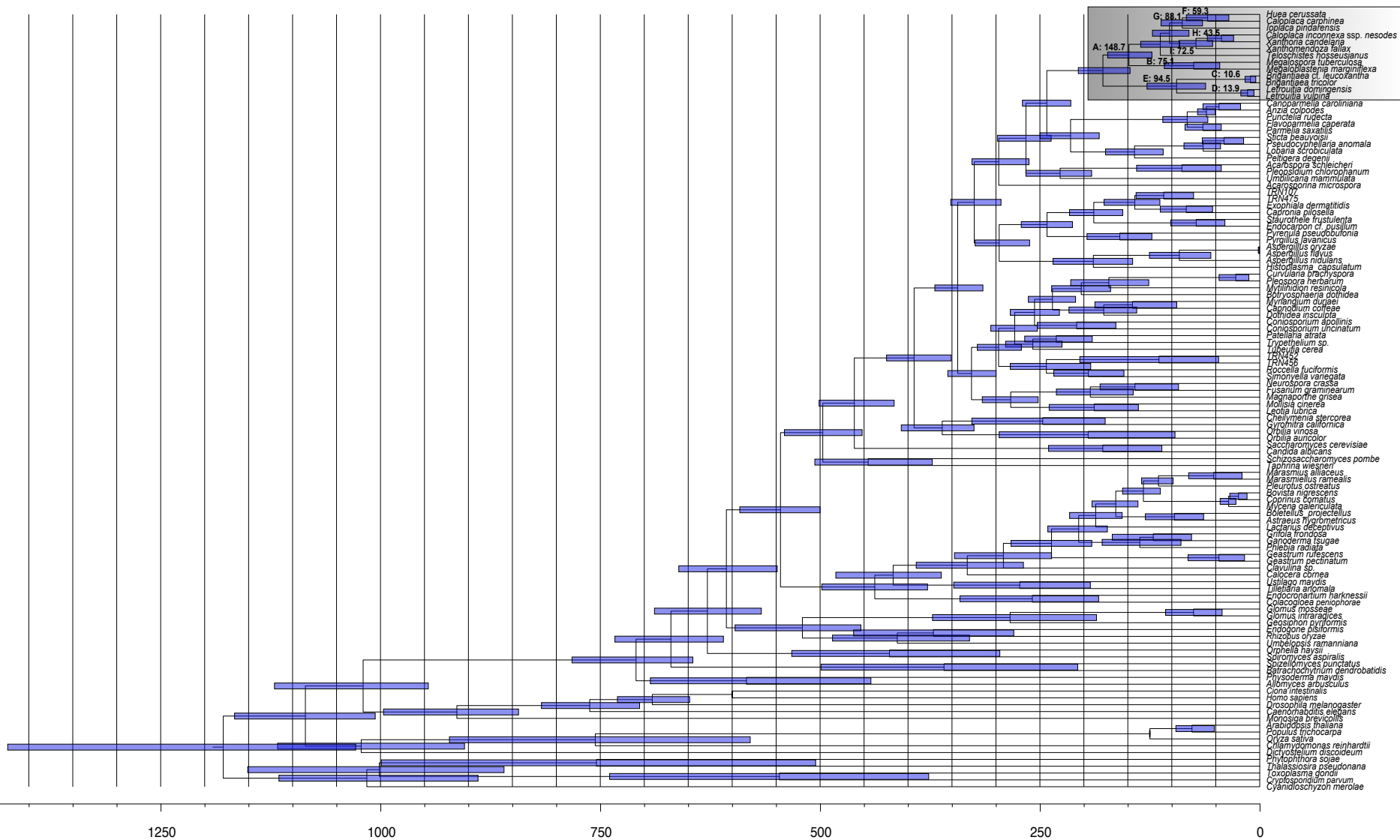


Fig. S6. Chronogram picturing divergence time estimates for 114 taxa representing all main groups of fungi and other eukaryotes (eukaryotes dataset) obtained using a five-gene dataset (*RPB1*, *RPB2*, *EF1a*, nrLSU, and nrSSU). Bars correspond to 95% confidence intervals. The Teloschistales clade is highlighted by a grey box.

Table S1. Summary of likelihood-ratio tests and Δ AICs of two alternative BiSSE models (full model versus $\lambda_0=\lambda_1$, $\mu_0=\mu_1$) considering different taxon sampling scenarios, with P-values based on a χ^2 distribution (16). Parameters were estimated using a single ML tree. (***) $p<0.001$, (**) $p<0.01$, (*) $p<0.05$).

BiSSE			
Anthra Thallus	ΔInL	ΔAIC	P value
Complete sampling	2.45	0.9	0.08678
90% Taxa sampled	2.66	1.4	0.07005
80% Taxa sampled	2.89	1.8	0.05564
70% Taxa sampled	3.07	2.2	0.0463 *
60% Taxa sampled	3.17	2.4	0.04173 *
50% Taxa sampled	3.18	2.4	0.0414 *
40% Taxa sampled	3.18	2.4	0.04139 *
30% Taxa sampled	3.18	2.4	0.04139 *
20% Taxa sampled	3.18	2.4	0.04139 *
10% Taxa sampled	3.18	2.4	0.0414 *
Anthraquinones	ΔInL	ΔAIC	P value
Complete sampling	3.18	2.37	0.04153 *
90% Taxa sampled	3.81	3.62	0.02219 *
80% Taxa sampled	4.06	4.11	0.01726 *
70% Taxa sampled	3.44	2.88	0.03214 *
60% Taxa sampled	3.48	2.95	0.0309 *
50% Taxa sampled	3.49	2.98	0.03047 *
40% Taxa sampled	3.49	2.98	0.03048 *
30% Taxa sampled	3.49	2.97	0.03057 *
20% Taxa sampled	3.49	2.99	0.03042 *
10% Taxa sampled	2.83	1.65	0.05899
Shade	ΔInL	ΔAIC	P value
Complete sampling	5.56	7.1	0.003869 **
90% Taxa sampled	5.95	7.9	0.002602 **
80% Taxa sampled	6.21	8.4	0.002007 **
70% Taxa sampled	6.62	9.2	0.001334 **
60% Taxa sampled	6.99	9.9	0.0009263 ***
50% Taxa sampled	7.25	10.5	0.0007091 ***
40% Taxa sampled	7.33	10.6	0.0006568 ***
30% Taxa sampled	7.33	10.6	0.0006594 ***
20% Taxa sampled	7.33	10.6	0.0006567 ***
10% Taxa sampled	7.33	10.6	0.0006569 ***
Rock	ΔInL	ΔAIC	P value
Complete sampling	2.01	0.1	0.1338
90% Taxa sampled	2.13	0.3	0.1177
80% Taxa sampled	2.27	0.5	0.1032
70% Taxa sampled	2.36	0.7	0.0947
60% Taxa sampled	2.37	0.8	0.09291
50% Taxa sampled	2.37	0.8	0.0929
40% Taxa sampled	2.38	0.8	0.09289
30% Taxa sampled	2.37	0.8	0.09289
20% Taxa sampled	2.37	0.8	0.09295
10% Taxa sampled	2.38	0.8	0.09528
Bark	ΔInL	ΔAIC	P value
Complete sampling	2.38	0.7	0.09173
90% Taxa sampled	2.57	1.2	0.07593
80% Taxa sampled	2.78	1.6	0.06203
70% Taxa sampled	2.94	1.9	0.05295
60% Taxa sampled	3.02	2.1	0.04885 *
50% Taxa sampled	3.02	2.1	0.04876 *
40% Taxa sampled	3.02	2.1	0.04875 *

Table S1. (Continued)

Bark	ΔlnL	ΔAIC	P value
30% Taxa sampled	3.02	2.1	0.04874 *
20% Taxa sampled	3.02	2.1	0.04877 *
10% Taxa sampled	3	2	0.04987 *
Crustose-continuous	ΔlnL	ΔAIC	P value
Complete sampling	8.06	12.1	0.0003149 ***
90% Taxa sampled	8.22	12.4	0.0002698 ***
80% Taxa sampled	8.38	12.7	0.0002282 ***
70% Taxa sampled	8.5	13	0.0002032 ***
60% Taxa sampled	8.55	13.1	0.000194 ***
50% Taxa sampled	8.55	13.1	0.0001941 ***
40% Taxa sampled	8.55	13.1	0.0001942 ***
30% Taxa sampled	8.54	13.1	0.0001943 ***
20% Taxa sampled	8.54	13.1	0.0001947 ***
10% Taxa sampled	8.54	13.1	0.000194 ***
Attach. Struct.	ΔlnL	ΔAIC	P value
Complete sampling	0.67	-2.6	0.5123
90% Taxa sampled	0.83	-2.3	0.4391
80% Taxa sampled	0.99	-2	0.3728
70% Taxa sampled	1.09	-1.8	0.3381
60% Taxa sampled	1.1	-1.8	0.3344
50% Taxa sampled	0.89	-2.2	0.4117
40% Taxa sampled	1.1	-1.8	0.3343
30% Taxa sampled	1.1	-1.8	0.3342
20% Taxa sampled	1.1	-1.8	0.3348
10% Taxa sampled	1.1	-1.8	0.3343

Table S2. Summary of likelihood-ratio tests and Δ AICs of alternative BiSSEness models (21) considering different taxon sampling scenarios. Parameters were estimated using a single ML tree. (***) $p < 0.001$, ** $p < 0.01$, * $p < 0.05$). The cases where a cladogenetic effect was significant are highlighted in red.

BiSSEness			
Anthra Thallus	ΔInL	ΔAIC	P value
Complete sampling:			
Full model vs. $p_{0c}=p_{1c}$	0.66	-0.7	0.2492
Full model vs. $p_{1c}=0$ ($p_{0c}=p_{1c}$)	1.19	-1.6	0.3038
Full model vs. $\lambda_0=\lambda_1, \mu_0=\mu_1$	1.35	-1.3	0.2581
$p_{0c}=p_{1c}$ vs. $p_{1c}=0$	0.53	-0.9	0.3044
$p_{1c}=0$ vs. $\lambda_0=\lambda_1, \mu_0=\mu_1$	2.45	0.9	0.08684
full model vs. $\lambda_0=\lambda_1, \mu_0=\mu_1$ ($p_{1c}=0$)	3.64	-0.7	0.1223
50% Taxa sampled:			
Full model vs. $p_{0c}=p_{1c}$	0.29	-1.4	0.4456
Full model vs. $p_{1c}=0$ ($p_{0c}=p_{1c}$)	0.87	-2.3	0.4201
Full model vs. $\lambda_0=\lambda_1, \mu_0=\mu_1$	2.5	1	0.08203
$p_{0c}=p_{1c}$ vs. $p_{1c}=0$	0.58	-0.9	0.283
$p_{1c}=0$ vs. $\lambda_0=\lambda_1, \mu_0=\mu_1$ ($p_{1c}=0$)	3.18	2.4	0.04142 *
Full model vs. $\lambda_0=\lambda_1, \mu_0=\mu_1$ ($p_{1c}=0$)	4.05	0.1	0.08789
10% Taxa sampled:			
Full model vs. $p_{0c}=p_{1c}$	0.04	-1.9	0.7797
Full model vs. $p_{1c}=0$ ($p_{0c}=p_{1c}$)	0.21	-3.6	0.813
Full model vs. $\lambda_0=\lambda_1, \mu_0=\mu_1$	3.09	2.2	0.04557 *
$p_{0c}=p_{1c}$ vs. $p_{1c}=0$	0.17	-1.7	0.5622
$p_{1c}=0$ vs. $\lambda_0=\lambda_1, \mu_0=\mu_1$ ($p_{1c}=0$)	3.18	2.4	0.04141 *
full model vs. $\lambda_0=\lambda_1, \mu_0=\mu_1$ ($p_{1c}=0$)	3.39	-1.2	0.1478
Shade	ΔInL	ΔAIC	P value
Complete sampling:			
Full model vs. $p_{0c}=p_{1c}$	0.03	-1.9	0.8072
Full model vs. $p_{1c}=0$ ($p_{0c}=p_{1c}$)	5.52	7.1	0.004013 **
Full model vs. $\lambda_0=\lambda_1, \mu_0=\mu_1$	2.74	1.5	0.06493
$p_{0c}=p_{1c}$ vs. $p_{1c}=0$	5.49	9	0.0009227 ***
$p_{1c}=0$ vs. $\lambda_0=\lambda_1, \mu_0=\mu_1$ ($p_{1c}=0$)	5.56	7.1	0.003856 **
full model vs. $\lambda_0=\lambda_1, \mu_0=\mu_1$ ($p_{1c}=0$)	11.08	14.2	0.0001869 ***
50% Taxa sampled:			
Full model vs. $p_{0c}=p_{1c}$	0.93	-0.1	0.1729
Full model vs. $p_{1c}=0$ ($p_{0c}=p_{1c}$)	5.26	6.5	0.005236 **
Full model vs. $\lambda_0=\lambda_1, \mu_0=\mu_1$	6.89	9.8	0.00102 **
$p_{0c}=p_{1c}$ vs. $p_{1c}=0$	4.33	6.6	0.003276 **
$p_{1c}=0$ vs. $\lambda_0=\lambda_1, \mu_0=\mu_1$	7.19	10.4	0.0007517 ***
full model vs. $\lambda_0=\lambda_1, \mu_0=\mu_1$ ($p_{1c}=0$)	12.45	16.9	5.292e-05 ***
10% Taxa sampled:			
Full model vs. $p_{0c}=p_{1c}$	0.98	0	0.1605
Full model vs. $p_{1c}=0$ ($p_{0c}=p_{1c}$)	1.63	-0.7	0.1952
Full model vs. $\lambda_0=\lambda_1, \mu_0=\mu_1$	7.8	11.6	0.0004076 ***
$p_{0c}=p_{1c}$ vs. $p_{1c}=0$	0.65	-0.7	0.2545
$p_{1c}=0$ vs. $\lambda_0=\lambda_1, \mu_0=\mu_1$ ($p_{1c}=0$)	7.33	10.6	0.0006568 ***
full model vs. $\lambda_0=\lambda_1, \mu_0=\mu_1$ ($p_{1c}=0$)	8.96	9.9	0.001277 **
Rock	ΔInL	ΔAIC	P value
Complete sampling:			
Full model vs. $p_{0c}=p_{1c}$	0.95	-0.1	0.1678
Full model vs. $p_{1c}=0$ ($p_{0c}=p_{1c}$)	5.97	7.9	0.002575 **
Full model vs. $\lambda_0=\lambda_1, \mu_0=\mu_1$	2.04	0.1	0.13
$p_{0c}=p_{1c}$ vs. $p_{1c}=0$	5.02	8	0.001548 **
$p_{1c}=0$ vs. $\lambda_0=\lambda_1, \mu_0=\mu_1$ ($p_{1c}=0$)	2.01	0.1	0.1338
full model vs. $\lambda_0=\lambda_1, \mu_0=\mu_1$ ($p_{1c}=0$)	7.98	8	0.003092 **

Table S2. (Continued).

Rock	$\Delta\ln L$	ΔAIC	P value
50% Taxa sampled:			
Full model vs. $p0c=p1c$	0.44	-1.1	0.3481
Full model vs. $p1c=0$ ($p0c=p1c$)	5.09	6.1	0.006191 **
Full model vs. $\lambda0=\lambda1, \mu0=\mu1$	3.26	2.5	0.03868 *
$p0c=p1c$ vs. $p1c=0$	4.65	7.2	0.002305 **
$p1c=0$ vs. $\lambda0=\lambda1, \mu0=\mu1$	2.37	0.8	0.09289
full model vs. $\lambda0=\lambda1, \mu0=\mu1$ ($p1c=0$)	7.46	6.9	0.004866 **
10% Taxa sampled:			
Full model vs. $p0c=p1c$	0.06	-1.9	0.7355
Full model vs. $p1c=0$ ($p0c=p1c$)	1.53	-1	0.2165
Full model vs. $\lambda0=\lambda1, \mu0=\mu1$	2.72	1.4	0.06545
$p0c=p1c$ vs. $p1c=0$	1.47	0.9	0.08606
$p1c=0$ vs. $\lambda0=\lambda1, \mu0=\mu1$ ($p1c=0$)	2.38	0.8	0.09287
full model vs. $\lambda0=\lambda1, \mu0=\mu1$ ($p1c=0$)	3.91	-0.2	0.09865
Bark	$\Delta\ln L$	ΔAIC	P value
Complete sampling:			
Full model vs. $p0c=p1c$	0.12	-1.7	0.6255
Full model vs. $p1c=0$ ($p0c=p1c$)	4.68	5.4	0.009305 **
Full model vs. $\lambda0=\lambda1, \mu0=\mu1$	3.2	2.4	0.04086 *
$p0c=p1c$ vs. $p1c=0$	4.56	7.1	0.002534 **
$p1c=0$ vs. $\lambda0=\lambda1, \mu0=\mu1$ ($p1c=0$)	2.38	0.7	0.09169
full model vs. $\lambda0=\lambda1, \mu0=\mu1$ ($p1c=0$)	7.06	6.1	0.006882 **
50% Taxa sampled:			
Full model vs. $p0c=p1c$	0.29	-1.4	0.4406
Full model vs. $p1c=0$ ($p0c=p1c$)	4.35	4.7	0.01283 *
Full model vs. $\lambda0=\lambda1, \mu0=\mu1$	3.89	3.8	0.02044 *
$p0c=p1c$ vs. $p1c=0$	4.06	6.1	0.004384 **
$p1c=0$ vs. $\lambda0=\lambda1, \mu0=\mu1$	3.02	2.1	0.04869 *
full model vs. $\lambda0=\lambda1, \mu0=\mu1$ ($p1c=0$)	7.37	6.8	0.005233 **
10% Taxa sampled:			
Full model vs. $p0c=p1c$	0.14	-1.7	0.5948
Full model vs. $p1c=0$ ($p0c=p1c$)	1.66	-0.7	0.1905
Full model vs. $\lambda0=\lambda1, \mu0=\mu1$	3.41	2.8	0.03312 *
$p0c=p1c$ vs. $p1c=0$	1.52	1	0.08158
$p1c=0$ vs. $\lambda0=\lambda1, \mu0=\mu1$ ($p1c=0$)	3.02	2.1	0.04873 *
full model vs. $\lambda0=\lambda1, \mu0=\mu1$ ($p1c=0$)	4.68	1.4	0.05273
Crustose-continuous	$\Delta\ln L$	ΔAIC	P value
Complete sampling:			
Full model vs. $p0c=p1c$	0.96	-0.1	0.1645
Full model vs. $p1c=0$ ($p0c=p1c$)	0.96	-2.1	0.3818
Full model vs. $\lambda0=\lambda1, \mu0=\mu1$	6.02	8	0.002411 **
$p0c=p1c$ vs. $p1c=0$	0	-2	-0.0070079
$p1c=0$ vs. $\lambda0=\lambda1, \mu0=\mu1$ ($p1c=0$)	8.06	12.1	0.0003149 ***
full model vs. $\lambda0=\lambda1, \mu0=\mu1$ ($p1c=0$)	9.02	10	0.001206 **
50% Taxa sampled:			
Full model vs. $p0c=p1c$	0.6	-0.8	0.2717
Full model vs. $p1c=0$ ($p0c=p1c$)	0.6	-2.8	0.5463
Full model vs. $\lambda0=\lambda1, \mu0=\mu1$	7.39	10.8	0.0006186 ***
$p0c=p1c$ vs. $p1c=0$	0	-2	0.9733
$p1c=0$ vs. $\lambda0=\lambda1, \mu0=\mu1$	8.55	13.1	0.0001942 ***
full model vs. $\lambda0=\lambda1, \mu0=\mu1$ ($p1c=0$)	9.15	10.3	0.001077 **
10% Taxa sampled:			
Full model vs. $p0c=p1c$	0.41	-1.1	0.3655
Full model vs. $p1c=0$ ($p0c=p1c$)	0.39	-3.2	0.6735

Table S2. (Continued).

Crustose-continuous	$\Delta\ln L$	ΔAIC	P value
Full model vs. $\lambda_0=\lambda_1, \mu_0=\mu_1$	8.52	13.1	0.0001995 ***
$p_{0c}=p_{1c}$ vs. $p_{1c}=0$	-0.02	-2.1	-0.028563
$p_{1c}=0$ vs. $\lambda_0=\lambda_1, \mu_0=\mu_1$ ($p_{1c}=0$)	8.55	13.1	0.000194 ***
full model vs. $\lambda_0=\lambda_1, \mu_0=\mu_1$ ($p_{1c}=0$)	8.94	9.9	0.001299 **
Attach. Struct.	$\Delta\ln L$	ΔAIC	P value
Complete sampling:			
Full model vs. $p_{0c}=p_{1c}$	0.91	-0.2	0.1763
Full model vs. $p_{1c}=0$ ($p_{0c}=p_{1c}$)	2.92	1.8	0.05394
Full model vs. $\lambda_0=\lambda_1, \mu_0=\mu_1$	2.18	0.3	0.1133
$p_{0c}=p_{1c}$ vs. $p_{1c}=0$	2.01	2	0.0452 *
$p_{1c}=0$ vs. $\lambda_0=\lambda_1, \mu_0=\mu_1$ ($p_{1c}=0$)	0.67	2.6	0.5122
full model vs. $\lambda_0=\lambda_1, \mu_0=\mu_1$ ($p_{1c}=0$)	3.59	-0.8	0.1268
50% Taxa sampled:			
Full model vs. $p_{0c}=p_{1c}$	1.36	0.7	0.09856
Full model vs. $p_{1c}=0$ ($p_{0c}=p_{1c}$)	2.44	0.9	0.0867
Full model vs. $\lambda_0=\lambda_1, \mu_0=\mu_1$	2.55	1.1	0.07797
$p_{0c}=p_{1c}$ vs. $p_{1c}=0$	1.08	0.2	0.1415
$p_{1c}=0$ vs. $\lambda_0=\lambda_1, \mu_0=\mu_1$	1.1	-1.8	0.335
full model vs. $\lambda_0=\lambda_1, \mu_0=\mu_1$ ($p_{1c}=0$)	3.54	0.1	0.1318
10% Taxa sampled:			
Full model vs. $p_{0c}=p_{1c}$	0.06	-1.9	0.728
Full model vs. $p_{1c}=0$ ($p_{0c}=p_{1c}$)	0.42	-3.2	0.6565
Full model vs. $\lambda_0=\lambda_1, \mu_0=\mu_1$	1.07	-1.9	0.3436
$p_{0c}=p_{1c}$ vs. $p_{1c}=0$	0.36	-1.3	0.3959
$p_{1c}=0$ vs. $\lambda_0=\lambda_1, \mu_0=\mu_1$ ($p_{1c}=0$)	0.94	-2.1	0.3941
full model vs. $\lambda_0=\lambda_1, \mu_0=\mu_1$ ($p_{1c}=0$)	1.36	-5.3	0.6085

Table S3. Voucher information for taxa included in this study organized according to the classification by (2). GenBank ID numbers are provided for sequences retrieved directly from GenBank, whereas GenBank accession numbers are provided for new sequences obtained in this study (indicated in bold). Sequences of *RPB2* are divided into two amplicons (5–7, 7–11). Asterisks indicate amplicons of *RPB2* newly sequenced in this study. In the Source column GB refers to GenBank as a source of sequences, and AFToL followed by numbers refer to the AFToL database.

Classification	Taxon	Source	Locality/ Voucher	ITS	mtSSU	nrLSU	<i>RPB1</i> [A-D]	<i>RPB2</i> [5-7]	<i>RPB2</i> [7-11]
Letrouitineae									
Brigantiaaceae	<i>Brigantiaea cf. leucoxantha</i>	GB/This study	Mascarene Islands, La Réunion, SW of St-André, N edge of Forêt Domaniale de la Plaine des Lianes, E-W trail, S of Cascade du Chien to Abri, boulders and outcrops in stream 'Bras des Lianes', tropical forest, 55°36.7'E 21°01.7'S, 730 m elev., on Guave, 5.6.2008, leg. P. & B. v.d. Boom 40691, D. & M. Brand, E. Sérusiaux (P.v.d. Boom Herb.).	394998679	394998502	394998567	394998728	KT291611	—
	<i>Brigantiaea fuscolutea</i>	GB	USA, Alaska, N of Skagway, White Pass, alpine, 59°36.833'N, 135°09.003'W, 948 m elev., over rocks on detritus in dry snow bed, 1.8.2008, leg. T. Sprillie 26961 (GZU).	—	394998503	394998569	394998732	—	394998802
	<i>Brigantiaea tricolor</i>	GB/This study	Mascarene Islands, La Réunion, NW of Plaine-des-Palmistes, NW side of Forêt de Bébour, trail GR R1 from Gîte de Bélouve, c. 3.5km to the south-west, to Caverne Mussard, 1980 m elev., well-lit area with mixed shrubs, including <i>Philippia</i> sp., on <i>Phyllia</i> sp., 2.6.2008, leg. P. & B. v.d. Boom 40492, D. & M. Brand & E. Sérusiaux (P.v.d. Boom Herb.).	394998680	—	394998568	394998730	394998800*	394998800
Letrouitiaceae	<i>Letrouitia domingensis</i>	GB	Dominican Republic, Duarte prov., NE of San Francisco de Macoris, Reserva Científica, SSE slope of Loma Quita Espuela, starting point at 'Rancho Don Lulu', trail in cocoa plantation with mature trees, 70°08.80'W 19°20.43'N, 400 m elev., on coffee shrub, 4.2.2008, leg. P. & B. v.d. Boom 39385 (P.v.d. Boom Herb.).	394998698	394998530	394998594	394998760	394998850	394998850
	<i>Letrouitia parabola</i>	GB	Alabama, Escambia Co., Andalusia Area, Solon-Dixon Forestry Center, montane rainforest, on <i>Fagus americana</i> , 14.4.2007, leg. E. Gaya 11 (DUKE).	394998700	394998532	394998595	394998762	—	394998852
	<i>Letrouitia vulpina</i>	GB	Mascarene Islands, La Réunion, Cirque de Cilaos, N of Cilaos, Forêt du Grand Matarum, trail GR R1, to Caverne Dufour, tropical rainforest, first part, from parking lot along road to Bras sec, up to 200 m in the forest, 55°29.2'E 21°07.3'S, 1420 m elev., on strong sloping trunk, 31.5.2008, leg. P. & B. v.d. Boom 40279, D. & M. Brand & E. Sérusiaux (P.v.d. Boom Herb.).	394998702	394998534	394998596	394998764	—	394998854
Teloschistineae									
Megalosporaceae	<i>Megaloblastenia marginiflexa</i>	GB/This study	Mascarene Islands, La Réunion, NW of Plaine-des-Palmistes, N side of Forêt de Bébour, Forêt de Bélouve (W), near Gîte de Bélouve, 55°32.50'E 21°03.50'S, 1520 m elev., area with mature <i>Acacia heterophylla</i> trees in mixed forest along road and path, on small tree, 27.5.2008, leg. P. & B. v.d. Boom 39805, D. & M. Brand & E. Sérusiaux (P.v.d. Boom Herb.).	394998703	394998535	394998597	394998766	394998856*	394998856
	<i>Megalospora coccodes</i>	This study	Mascarene Islands, La Réunion, Cirque de Cilaos, N of Cilaos, Forêt du Grand Matarum, trail GR R1, to Caverne Dufour, tropical rainforest, first part, from parking lot along road to Bras sec, up to 200 m in the forest, 55°29.2'E 21°07.3'S, 1420 m, on unidentified tree, 8 cm diam, 31.5.2008, leg. P. & B. v.d. Boom 40221, D. & M. Brand & E. Sérusiaux (P.v.d. Boom Herb.).	KT291469	KT291520	KT291563	—	—	—

	<i>Megalospora sulphurata</i>	GB	Mascarene Islands, La Réunion, NW of Plaine-des-Palmistes, Forêt de Bébou, trail in tropical rainforest, from main road, just N of Col de Bébou, to Cassé de Takamaka, 1340 m elev., on Dombeya, 1.6.2008, leg. P. v.d. Boom 40349, M. Brand & E. Sérusiaux (P.v.d. Boom Herb.).	394998706	394998539	394998598	—	—	394998858
	<i>Megalospora tuberculosa</i>	GB/AFToL-107	Costa Rica, Puntarenas, Zona Protectora Las Tablas (AC Amistad Pacifico), Los Portones, 25 km ENE of San Vito, 5 km on gravel road from Progreso to Las Tablas, road side, 82° 48'W 8°55'N, 1600 m elev., 28.6.2002, leg. H. Sipman 47933 (DUKE).	336397114	46411388	46411439	113707385	113957833	113957833
	<i>Sipmaniella sulphureofusca</i>	GB/This study	Ecuador, Zamora-Chinchi, Nature Reserve of Estación Científica San Francisco, S of road Loja-Zamora, ca. 40 km from Loja, 79°04'W 3°58'S, 1945 m elev., primary montane forest on steep slope, <i>Prunus huantensis</i> , on canopy, 2.7.2004, leg. H. Sipman 53087 (B).	—	394998529	394998593	—	KT291659	—
Teloschistaceae (Caloplacoideae)	<i>Caloplaca aegaea</i>	GB/This study	Spain, Catalonia, Girona prov., Alt Empordà, Llança, Cau del Llop, wall facing North, slope 10°-30°, 3-5 m, 11.01.2001, leg. E. Gaya 248 & X. Llimona.	183585217	—	—	—	KT291612	KT291612
	<i>Caloplaca aetnensis</i>	GB/This study	Spain, Catalonia, Girona prov., Alt Empordà, Castell de Quermançó (Vilajuïga), facing South, slope 80°, weathered granite, 23.01.2001, leg. X. Llimona s.n. (BCN).	183585210	KT291476	—	—	—	KT291613
	<i>Caloplaca atroflava</i>	This study	USA, California, Sta Cruz Island, along road linking the duck and the ranch along river, open oak forest, 34°0.017'N 119°45.097'W, 46 m, shady, 25° slope, very humid, rock immediately bordering a small creek, semi-aquatic, leg. E. Gaya 02.27.10-8a & F. Lutzoni (DUKE).	KT291444	KT291511	KT291560	KT291593	KT291650	KT291650
	<i>Caloplaca aurantia</i>	GB/This study	Spain, Catalonia, Lleida prov., Segarra, Torà, slopes in the right side of the road to Solsona, Km 13, in front of Sant Miquel de Fontanet church, 41°49'20"N 1°25'10"E, 31TCG6831, 450-550 m, blocks of carbonated sandstone, <i>Quercus faginea</i> brushwood, 23.02.1999, leg. P. Navarro-Rosinés & X. Llimona s.n. (BCN 13326).	183585222	KT291479	—	—	KT291616	KT291616
	<i>Caloplaca cancarixitcola</i>	GB/This study	Spain, Castilla-La Mancha, Albacete prov., between Agramón and Cáncarix (Sierra de las Cabras), 30SXH2353, 671 m, on cancarixite, 03.1981, leg. X. Llimona & J.M. Egea s.n. (MUB, holotype).	183585228	KT291482	—	—	KT291620	KT291620
	<i>Caloplaca carphinea</i>	GB/This study	Spain, Catalonia, Girona prov., Alt Empordà, P.N. Cap de Creus, Roses, near Puig del Gall, above Mas de la Torre del Sastre, Jóncols road, 31TEG1777, 200-300 m elev., quartzite blocks, 11.1.2001, leg. E. Gaya 201, X. Llimona & M. De Cáceres (BCN 13714).	183585215	—	—	—	KT291621	—
		GB	Spain, Catalonia, Girona prov., Alt Empordà, P.N. Cap de Creus, Roses, near Puig del Gall, above Mas de la Torre del Sastre, Jóncols road, 31TEG1777, 200-300 m elev., siliceous rocks (quartzite), 4.1.2008, leg. E. Gaya, S. Fernández-Brime 542 & X. Llimona (BCN).	—	394998507	394998573	394998736	—	394998808
	<i>Caloplaca catalinae</i>	This study	USA, California, Sta. Cruz Island, South ridge road, 34°00.542'N 119°46.934'W, 405 m, <i>Quercus pacifica</i> forest/shrub, very exposed to light, flat, on branches of dead scrub oaks, leg. E. Gaya 02.26.10-13 & F. Lutzoni (DUKE).	KT291445	KT291477	KT291532	KT291572	—	KT291614
	<i>Caloplaca cerina</i>	GB	USA, Alaska, Elliott Hwy, N65°17.229' W148°11.537', 400 m elev., ca. mile 40, on aspen, 22.7.2007, leg. E. Gaya, J. Geml, J. Gomà (DUKE).	—	394998508	394998574	—	394998810	—
	<i>Caloplaca chalybaea</i>	GB/This study	Sweden, Gotland, Östergarn par., Österganberget, 57°25'30"N 18°50'24"E, 33 m elev., on calcareous rocks, 14.8.2006, leg. E. Gaya, P. Navarro-Rosinés, U. Arup, U. Sochting, N. Hladun, A. Gómez-Bolea (BCN).	394998684	394998509	394998575	394998738	394998812*	394998812
	<i>Caloplaca chlorina</i>	This study	Sweden, Skåne, Genarp par., Genarp church, at the parking place W of the churchyard. On <i>Fraxinus</i> in open, nutrient-enriched situation, RT90: X 6166399 Y 1348136, 09/05/2009, Leg. Ulf Arup L09009 (LD).	KT291449	KT291483	—	KT291576	KT291622	—

<i>Caloplaca cinnamomea</i>	GB	Iceland, Sudur-Thingeyjarsýsla County, Laxardalur Valley, by Laxa river close to abandoned farm Brettingsstadir, 65°38'24"N, 17°09'48"W, on mosses on soil on big lava extrusion, about 50 m from river, 8.6.2006, leg. F. Lutzoni & C. Gueidan 06.08.07-1 (DUKE).	—	394998512	394998577	394998742	—	394998818
<i>Caloplaca conversa</i>	This study	Mexico, Baja California South, Loreto, Sierra Giganta, on the road from Loreto to San Javier, next to cinegetic ranch, on plateau, after las parras, 25°57.099'N 111°30.984'W, 514 m, leguminose shrubs and cactus, open-exposed site, North exposure, basaltic boulder along dry creek, leg. E. Gaya 03.03.10-2C & F. Lutzoni (DUKE).	KT291450	KT291504	KT291554	KT291589	KT291643	KT291643
<i>Caloplaca crenularia</i>	GB	Sweden, Bohuslän, Kungshamn par., Sunnerskär, 58°19'42.53"N 11°14'48.12"E, 5 elev., granitic islands, 11.8.2006, leg. E. Gaya, P. Navarro-Rosinés, U. Arup, U. Sochting, N. Hladun, A. Gómez-Bolea (BCN).	394998686	394998514	—	394998744	—	394998822
<i>Caloplaca flavorubescens</i>	GB	We6140; Kasalicky T., Doering H., Rambold G. and Wedin M. (2000).	13810817	—	13810817	—	—	—
	GB	Wedin M., Baloch E. and Grube M. (2002); Wedin M., Doring H., Nordin A. and Tibell L. (2000).	—	33304587	—	—	—	—
<i>Caloplaca glorieae</i>	GB	Spain, Almería, E-SE of Almería, Sierra del Cabo de Gata, SW San José, path between Casa Mónsul to Torre de Vela Blanca, small valley (N-S), NE exposed sloping outcrops, 2°10.14'W 36°43.85'N, 75 m elev., volcanic outcrops, 6.9.2007, leg. P. & B. v.d. Boom 38420 (P.v.d. Boom Herb.).	—	—	394998580	394998746	394998826	394998826
<i>Caloplaca isidiigera</i>	GB/This study	Slovakia, Low Tatras mountains, eastern part of mountains range, mount Velký bok, small limestone outcrops near tourist trail on south slope, 48°56'03.35"N 19°52'53.44"E, 1560 m elev., limestone outcrops, 14.8.2007, leg. J. Šoun (CBFS).	KT291460	394998517	394998581	394998748	394998828*	394998828
<i>Caloplaca paulii</i>	GB/This study	Spain, Catalonia, Girona prov., Ripollès, Queralbs, Vall de Núria, entre el Torrent de Noucreus i la Coma de les Mulleres, 31TDG3195-3295, 2200-2400 m, decalcified surfaces of calcareous schist, facing North-West, 02.09.2000, leg. E. Gaya 183 (BCN).	183585226	KT291503	—	—	KT291642	KT291642
<i>Caloplaca pelloidella</i>	This study	Mexico, Baja California South, Loreto, Sierra Giganta, on the road from Loreto to San Javier, next to cinegetic ranch, on plateau, after las parras, 25°57.099'N 111°30.984'W, 514 m, leguminose shrubs and cactus, open-exposed site, North exposure, basaltic boulder along dry creek, leg. E. Gaya 03.03.10-2A & F. Lutzoni (DUKE).	—	KT291505	KT291555	KT291590	KT291644	KT291644
<i>Caloplaca proteus</i>	GB/This study	Spain, Catalonia, Tarragona prov., Conca de Barberà, Vimbodí, la Pena (Serra de Prades), 31TCF4181-4281, 700-900 m, walls and small caves of carbonated rocks, NE exposure, 18.01.2001, leg. E. Gaya 215 & X. Limona (BCN 13706).	183585233	KT291507	KT291557	—	KT291646	KT291646
<i>Caloplaca scoriophila</i>	GB/This study	Spain, Almería, E-SE of Almería, Sierra del Cabo de Gata, path W of Torre de Vela Blanca to lighthouse, small hill, NE exposed sloping outcrops, 2°10.46'W 36°43.82'N, 150 m elev., 6.9.2007, leg. P. & B. v.d. Boom 38386 (P. v.d. Boom Herb.).	394998689	394998521	394998585	394998750	394998832*	394998832
<i>Caloplaca scotoplaca</i>	GB/This study	Sweden, Bohuslän, Askums par., Vägga, Lökås, near Kugshamn, 58°21'58.36"N 11°17'01.19"E, 22 m elev., siliceous rocks, 11.8.2006, leg. E. Gaya, P. Navarro-Rosinés, U. Arup, U. Sochting, N. Hladun, A. Gómez-Bolea (BCN).	394998690	394998522	394998586	394998752	394998834*	394998834
<i>Caloplaca stillicidiorum</i>	GB/This study	France, Rhône-Alpes, Haute-Savoie Platcau des Glières - la Commanderie, palaise au NE de la Mison de paps 1500 m, 90°S, calcareous.	183585227	KT291510	—	—	—	KT291649
<i>Caloplaca stipitata</i>	This study	Mexico, Baja California South, along road between La Paz and La Constitución, closer to La Paz, 24°03.174'N 110°34.719'W, 268 m, leguminose with cactuses and <i>Yucca</i> , sun-exposed, flat slope, on an individual shrub, leg. E. Gaya 03.06.10-5 & F. Lutzoni (DUKE).	KT291465	KT291490	KT291543	KT291582	KT291630	KT291630

<i>Caloplaca teicholyta</i>	GB/This study	Spain, Catalonia, Lleida prov., Segarra, Torà, above Font de Can Porta, road to Solsona, 41°49'05"N 1°25'05"E, 31TCG6830, 550-650 m, sun-exposed blocks of calcareous sandstone, 01.09.2000, leg. E. Gaya 203 & P. Navarro-Rosinés (BCN 13695).	183585212	KT291512	—	KT291594	KT291651	KT291651
<i>Caloplaca thallicola</i>	GB/This study	Sweden, Halland, Varberg, Vendelsö island, 57°17'54.53"N 12° 07'29.68"E, 0-2 m elev., on siliceous rocks, 9.8.2006, leg. E. Gaya, P. Navarro-Rosinés, U. Arup, U. Sochting, N. Hladun, A. Gómez-Bolea (BCN).	394998692	394998523	394998588	KT291595	394998838*	394998838
<i>Caloplaca thracopontica</i>	GB	Turkey, Black Sea Coast, Sinop, coastal rocks on NE coast of peninsula, 42°01'57.81"N 35°11'34.42"E, 130 m elev., on volcanic rocks, 21.4.2007, leg. J. Soun (CBFS).	394998693	394998524	—	—	—	394998840
<i>Caloplaca variabilis</i>	This study	Italy, Veneto, Verona prov., N-NE of Verona, Monte Purga at Velo Veronese, S-facing grazed slope above the village. On limestone rocks. 45°36.755'N. 11°05.905'E, alt. C. 1230 m. 2007-03-08. Leg. Ulf Arup L07196 (LD).	KT291466	KT291514	KT291561	KT291597	KT291653	—
<i>Caloplaca velana</i>	This study	Italy, Veneto, Verona prov., San Giogio NE of Ambrogio di Valpolicella, SE-facing slope NE of Biotto. On limestone rocks in SE-facing slope with scattered bushes. 45°32.191'N 10°50.548'E, 380 m elev., 2007-03-09. Leg. Ulf Arup L07123 (LD).	KT291467	KT291515	—	KT291598	—	KT291654
<i>Caloplaca xantholyta</i>	GB/This study	Greece, Crete, Imbros Gorge, 24°09.5'E 35°14'N, 400-700 m elev., on calcareous rock walls, 7.5.2004, leg. T. Spribille 12970 (B).	394998695	394998526	394998590	—	394998844*	394998844
<i>Fulgensia bracteata</i>	GB	K141, Kasalicky T., Doering H., Rambold G. and Wedin M. (2000).	13810787	—	—	—	—	—
	GB/AFToL-4844	Estonia, Saaremaa, Sörve, Kaugatuma alvar, on dry places along road, on soil, 15.6.2004, leg. P. Alanko 121555 (H).	—	394998527	394998591	—	—	—
<i>Fulgensia canariensis</i>	GB/This study	Spain, Canary Islands, La Palma, summits of Caldera de Taburiente (Parque Nacional), 2200 m alt., 07.2001, leg. P.L. Pérez de Paz & C. Hernández-Padrón s.n. (TFC Lich: 3593, duplic.).	183585207	KT291516	KT291562	KT291599	KT291655	KT291655
<i>Fulgensia fulgens</i>	GB/This study	Sweden, Öland, Hulterstad par., 1.5 km WNW of Gösslunda, N from the road, 56°29'33.84"N 16°30'41.96"E, 33 m elev., calcareous soils and rocks (Ordovician), 12.8.2006, leg. E. Gaya, P. Navarro-Rosinés, U. Arup, U. Sochting, N. Hladun, A. Gómez-Bolea (BCN).	394998696	394998528	394998592	394998756	394998846*	394998846
<i>Fulgensia klementii</i>	This study	Turkey, Konya province, Geune Valley, Beyrelli village, N36°51'220" E32°21'905", 1560 m, on calcareous rocks, 28.07.2011, leg. M. Kocakaya and M. G. Halici.	KT291468	KT291517	—	KT291600	KT291656	KT291656
<i>Fulgensia poeltii</i>	GB/This study	Spain, Catalonia, Lleida prov., between Ponts i Torà, after the crossroad de Guissona, Mas d'en Bruc, entre Cal Perxa i Casanova de la Garriga, gypsum-rich walls, South exposure, 27.04.2002, leg. E. Gaya 400 (BCN).	183585206	KT291518	—	—	KT291657	—
<i>Huea cerussata</i>	This study	South America. Unknown locality, leg. Ulrik Sochting.	—	KT291519	—	KT291601	KT291658	KT291658
<i>Ioplaca pindarensis</i>	GB	China, Yunnan prov., Dali co., Mt. Cangshan, 3150-3500 m elev., sclerophyll shrub on steep mountains slopes, on shale, leg. A. Aptroot 56827 (ABL).	394998697	—	—	394998758	394998848	—
<i>Seiophora californica</i>	This study	Mexico, Baja California South, along road, between Ciudad Constitution and Puerto San Carlos, N25°02.337' W111°45.814', 41 m, shrubs, with legumes, cactuses, and <i>Fulqueria</i> , sun exposed site, flat, humid, on <i>Fulqueria</i> , leg. E. Gaya 03.04.10-9 & F. Lutzoni (DUKE).	KT291470	KT291521	KT291564	KT291602	KT291660	—
<i>Seiophora contortuplicata</i>	This study	Tajikistan, 4000m, 14.09.2010, leg. U. Sochting	KT291471	KT291522	—	KT291603	KT291661	—
<i>Seiophora lacunosa</i>	GB	Spain, Alacant, Les Salines d'Elda, at margins of seasonal lagoon, 30SXH86, 500 m elev., on soil, 28.3.2002, leg. A. Pérez s.n. (BCN, herb. Gaya 391).	394998708	394998542	394998600	394998770	394998864	394998864

(Teloschistoideae)	<i>Caloplaca brouardii</i>	Mexico, Baja California South, Loreto, Sierra La Giganta, on the road from Loreto to San Javier, next to cinegetic ranch, on plateau, after Las Parras, 25°57.099'N 111°30.984'W, 514 m, shrubs (leguminose) and cactus, sun-exposed, little cliff, facing creek N-NE, exposure North, slope 0-5° flat, substrate locality is volcanic-basaltic, sample collected in different rocks, less vitrified conglomerate, leg. E. Gaya 03.03.10-3 & F. Lutzoni (DUKE).	This study	KT291448	—	KT291536	KT291575	KT291619	KT291619
	<i>Caloplaca chilensis</i>	Chile, P.N. Fray Jorge, IVrta Región, 30°39'48"S 71°4'23.7", 455 m elev., on twigs, 5.2008, leg. D. Stanton 0212-0508 (SGO).	GB	394998685	394998510	394998576	394998740	—	394998814
	<i>Caloplaca chrysopteralma</i>	Mexico, Sonora, along road 14 to Moctezuma 29°37.009'N 109°56.934'W, 912 m, open forest, partially shaded, top of mountain, epiphytic on bark of the dominant tree, leg. E. Gaya 03.08.10-4 & F. Lutzoni (DUKE).	This study	KT291446	KT291484	KT291537	KT291577	KT291623	KT291623
	<i>Caloplaca cinnabarina</i>	Mexico, Baja California, along trail between La Burrera and La Laguna, 23°30.973'N 110°02.325'W, 680 m, legume small trees and cactus, 75% sun-exposed site, exposure W, slope 70°, west exposure, humid, on rock boulders along trail, leg. E. Gaya 03.05.10-11 & F. Lutzoni (DUKE).	This study	—	—	KT291538	KT291578	KT291624	KT291624
	<i>Caloplaca decipoides</i>	South Korea, Gangwon Province, Inje-gun, Buk-myun, Yongdae-ri, Sorak-san National Park, inner part of the massif Sorak Mts, along the road in Backdam Valley, from Backdam (Paekdam) temple towards the village Yongdae-ri, where the road crosses the river ca. 1.5 km NW Backdam (Paekdam) temple, 38°10'N 128°22'E, 410–420 m, on almost vertical rock, shaded from running water, probably at least partly with a higher pH than true siliceous rocks, exposed to S at the river, October 2006, Thor 20768 (holotype UPS, isotypes NIBR, UPS).	This study	KT291453	KT291487	KT291540	KT291579	KT291627	—
	<i>Caloplaca elegantissima</i>	Namibia, Skeleton coast, 2000, leg. P. Crittenden	This study	KT291454	KT291488	KT291541	KT291580	KT291628	KT291628
	<i>Caloplaca eos</i>	Australia, New South Wales, S of Anna Bay, Tomaree National Park, 32°47'16"S 152°44'48"E, rock (rhyolite) outcrops along the coast, 24.01.2004, Kärnefelt 20044701, Filson & Kondratyuk 20475 (CANB - holotype, PERTH, AQ, MEL, LD, KW - isotypes).	This study	KT291455	KT291489	KT291542	KT291581	—	KT291629
	<i>Caloplaca aff. luteoalba</i>	Mexico, Baja California South, along road between La Paz and La Constitución, closer to La Paz, 24°03.174'N 110°34.719'W, 268 m, leguminose with cactuses and <i>Yucca</i> , sun-exposed, on a legume tree about 5 m high leg. E. Gaya 03.06.10-7B & F. Lutzoni (DUKE).	This study	KT291447	KT291497	KT291550	—	—	KT291636
	<i>Caloplaca microphyllina</i>	USA, California, Sta Cruz Island, near main ranch on the road passing to the right of the church when facing the church, 33°59.672'N 119°42.627'W, 58 m, patch of very large <i>Quercus</i> , on fallen dead trees, leg. E. Gaya 02.27.10-24 & F. Lutzoni (DUKE).	This study	KT291462	KT291501	—	—	—	KT291639
	<i>Caloplaca santessoniana ad int.</i> (sub. <i>Caloplaca</i> sp. EG-2015a in GB)	Chile, Parque Nacional Pan de Azúcar, coastal hill crust, 25°59'05.7"S 70°36'51.2"W +/- 3 m, 720 m, leg. E. Gaya 19.2.11- 37 & R. Vargas (DUKE).	This study	KT291463	KT291508	KT291558	KT291592	KT291647	KT291647
	<i>Caloplaca</i> sp. 110	USA, California, Sta Cruz Island, along the road linking the duck and the ranch, along river, on open slope facing North, 33°59.955'N 119°42.8991'W, 46 m, oak forest, partly shady, slope 25°, volcanic rock, on creek, semi-aquatic, leg. E. Gaya 02.27.10-8B & F. Lutzoni (DUKE).	This study	KT291456	KT291499	KT291552	KT291587	KT291637	KT291637
	<i>Teloschistes chrysopteralmus</i>	Spain, Catalonia, Tarragona prov., Conca de Barberà, Vimbodi, Barranc de Castellfolit, 550-650 m elev., 31TCF3780-3781, on <i>Quercus ilex</i> ssp. <i>ballota</i> , 18.1.2001, leg. E. Gaya 200b & X. Llimona (BCN 13687).	GB	183585272	394998543	394998601	394998772	394998866	394998866
	<i>Teloschistes exilis</i>	USA, Texas, Mason co., Double Helix Ranch, 411 m elev., 30°52'28"N 99°02'53"W, 26.05.07, on bark, D. Hillis 07-726 (DUKE).	GB	394998709	394998544	394998602	394998774	394998868	394998868

<i>Teloschistes flavicans</i>	This study	USA, California, Sta Cruz Island, South Rigde road, 34°00.763'N 119°47.485'W, 422 m, Southern exposure, 45° slope, shrub oak vegetation, sun-exposed, on <i>Quercus pacifica</i> , young, on small branches, the oak was about 3' tall, leg. E. Gaya 02.26.10-8, F. Lutzoni (DUKE).	KT291472	KT291523	KT291565	KT291604	—	KT291662
<i>Teloschistes hosseusianus</i>	GB/This study	Argentina, Villaciencio, 1.12.2007, leg. W.F. Morris (DUKE).	394998711	394998546	394998604	394998778	394998872*	394998872
<i>Teloschistes nodulifer</i>	This study	Peru, Tarma province, Capia, above Tarma village, S11°25'12.3" W75°40'39", 3138 m, open-exposed site, 50-60° slope, dry desert, soil in small hills mixed with basaltic, leg. E. Gaya 07.05.10-7, D. Ramos (DUKE).	—	KT291524	KT291566	KT291605	KT291663	KT291663
<i>Teloschistes sieberianus</i>	GB/This study	Australia, New South Wales, secus viam ad "Coreys Cave" ducentem, 2 km ad septentriones et orientem a Wee Jasper (35°06' austr., 148°40' orient.), 400 m s. m. In ramulis silva (<i>Eucalyptus</i>), 12.08.1991, leg. H.T. Lumbsch & H. Streimann s.n. (DUKE, A. Vezda: Lichenes rarores exsiccati 30).	183585275	KT291525	—	—	KT291664	—
<i>Xanthoria andina</i>	GB	Bolivia, Dpto. La Paz, Prov. Murillo, Laguna de Cota – Cota (calle 31), sector frente a la puerta principal, 16°32'24.8"S 68°04'01.7"W, 3750 m elev., Puna and Altoandina vegetation, on <i>Populus balsamifera</i> , 8.2.2002, leg. Canseco A-113 (LPB-B).	394998717	394998557	394998616	—	394998894	394998894
(Xanthorioideae)								
<i>Caloplaca altoandina</i> (sub <i>C. squamosa</i> s.l. in GB)	GB/This study	Argentina, Villaciencio, 1.12.2007, leg. W. Morris (DUKE).	394998691	—	394998587	394998754	394998836*	394998836
<i>Caloplaca arnoldii</i> ssp. <i>obliterata</i>	GB	Sweden, Halland, Varberg, Vendelsö island, 57°17'54.53"N 12° 07'29.68"E, 0-2 m elev., on siliceous rocks, 9.8.2006, leg. E. Gaya, P. Navarro-Rosinés, U. Arup, U. Sochting, N. Hladun, A. Gómez-Bolea (BCN).	394998682	394998506	394998572	394998734	394998806	394998806
<i>Caloplaca bolacina</i>	GB/This study	Mexico, Baja California sur, Sta Rosalia - Guerrero Negro, Desierto de Vizcaino, Llano El Angel, N of San Ignacio, 3,5 km from highway 1 along road to punta Abreojos, 27°15'N 113°11'W, 60-260 m, volcanic rocks, 21.02.1993, leg. Pere Navarro-Rosinés (BCN-Lich 12532).	183585246	KT291480	KT291534	—	KT291617	KT291617
<i>Caloplaca coralloides</i>	This study	USA, California, Santa Barbara, San Miguel Island, secondary point at the beginning (N-side) of Harris Point, 34.07083(34°4'15"N)-120.35972 (120°21'35"W), 30 m (98ft), acidic rock, 15 March 1998, leg. T.H. Nash III 41158 (ASU 511740).	KT291451	KT291485	KT291539	—	KT291625	—
<i>Caloplaca coronata</i>	GB	Spain, Almería, ENE of Almería, N rim of Sierra Cabrera, W of Mojácar, W of Turre, road AL150, near bridge over Rio de Aguas, 1°55'97"W 37° 08'48"N, 90 m elev., N exposed rocky and grassy slope with some shrubs and <i>Chamareops humilis</i> , terricolous and mostly low outcrops, on vertical shaded low outcrop, 5.9.2007, leg. P. & B. v.d. Boom 38374 (P.v.d. Boom Herb.).	—	394998513	394998578	—	394998820	—
<i>Caloplaca crenulatella</i>	This study	USA, California, end of Morris Ranch Road above Cedar Springs Trail, 33°39.373'N 116°35.056'W, 1559 m, chaparral and yucca, completely open-exposed site, slope 50°, dry, on limestone, leg. E. Gaya 02.24.10-23 & F. Lutzoni (DUKE).	KT291452	KT291486	—	—	—	KT291626
<i>Caloplaca</i> aff. <i>durietzii</i>	This study	USA, California, Saint Jacinto mountains, Highway 74, on the other side of the road from, along the pacific crest trail, 4 1/2 from Table Mountain road, 33°33.753'N 116°34.649'W, 1493 m, desert chaparral, dry, sun-exposed, flat, on <i>Quercus</i> with leaves, Leg. E. Gaya 02.25.10-4 & F.Lutzoni (DUKE).	KT291442	KT291481	KT291535	KT291574	KT291618	KT291618
<i>Caloplaca granulosa</i>	GB/This study	Spain, Catalonia, Tarragona prov., Conca de Barberà, Vimbodí, la Pena (Serra de Prades), under l'Àliga peak, near Roca de les Abelles, 31TCF3980, 900-1000 m, rainwater runoff on calcareous vertical walls, 18.01.2001, leg. E. Gaya 223 & X. Llimona (BCN 13702).	183585250	KT291491	KT291544	KT291583	—	KT291631

<i>Caloplaca ignea</i>	This study	USA, California, Sta Cruz Island, along road linking the duck and the ranch along river, open oak forest, 34°0.017'N 119° 45.097'W, 46 m, shady, 25° slope, very humid, on small boulder embedded in soil about 1 m above water level of creek, leg. E. Gaya 02.27.10-9 & F. Lutzoni (DUKE).	KT291458	KT291492	KT291545	—	KT291632	KT291632
<i>Caloplaca impolita</i>	This study	USA, California, Sta Cruz Island, along road in Cristy Canyon, Centinella grave, 34°00.955'N 119°48.096'W, 330 m, Southern exposure, 70° slope, low shrub <i>Artemisia</i> and shrub oak, on volcanic rock, leg. E. Gaya 02.26.10-5 & F. Lutzoni (DUKE).	KT291459	KT291493	KT291546	KT291584	KT291633	KT291633
<i>Caloplaca inconnexa</i>	GB/This study	France, Provence, prov. De Bouches-du-Rhône, Mimet, Col d'Ange, 500 m E de Pilon-du-Roi, 600-670 m, calcareous rocks, parasite on <i>Aspicilia calcarea</i> (BCN 13375).	183585267	KT291494	KT291547	—	KT291634	—
<i>Caloplaca inconnexa</i> ssp. <i>nesodes</i>	This study	USA, California, Sta Cruz Island, along the road linking the duck and the ranch along river, 33°59.955'N 119°42.8991'W, 46 m, oak forest, slope 45°, volcanic rock, on terrace of a sunlit block, leg. E. Gaya 02.27.10-7 & F. Lutzoni (DUKE).	KT291457	KT291495	KT291548	KT291585	KT291635	KT291635
<i>Caloplaca luteoalba</i>	This study	Sweden, Halland, Övraby, Sperlingsholm, 56°42'28.96"N 12° 53'46.93"E, 32 m, epiphyte on <i>Ulmus glabra</i> , 9.8.2006, leg. E. Gaya, P. Navarro-Rosinés, U. Arup, U. Sochting, N. Hladun, A. Gómez-Bolea (BCN).	KT291461	KT291496	KT291549	KT291586	—	—
<i>Caloplaca</i> aff. <i>luteominia</i>	This study	USA, California, San Bernardino mountains, Cactus Flats, road 18, after Big Bear city, rocky hill, 34°18.879'N 116°48.495'W, 1863 m, Joshua tree with <i>Juniper</i> and oaks, 45° of slope, on granitic boulders, carbonated, on sides of rainwater runoff, leg. E. Gaya 02.23.10-17, F. Lutzoni (DUKE).	KT291443	KT291478	KT291533	KT291573	KT291615	KT291615
<i>Caloplaca marina</i>	GB	U. Arup and M. Grube (1999).	13242210	—	—	—	—	—
	GB/AFToL -4819	Finland, Uusimaa, Kirkkonummi, Porkkala, Vetokannas, 59°59'N 24°25'E, on bare seashore cliffs, 7.4.2005, leg. S. Stenroos 5686 (H).	—	394998518	394998582	—	—	—
<i>Caloplaca maritima</i>	GB/This study	Spain, Catalonia, Girona prov., Llança, Cau del Llop, surface facing North, 10°-30° slope, 3-5 m, 11.01.2001, leg. E. Gaya 243b & X. Llimona (BCN).	183585247	KT291498	KT291551	—	—	—
<i>Caloplaca marmorata</i>	GB/This study	France, Provence, Var, Massif de la Ste. Baume, Plan d'Aups, entre l'Hostellerie de la Ste. Baume et le Vallon de Castelette, sun-exposed calcareous rocks, 10.06.2002, leg. E. Gaya 416 & C. Gueidan (BCN).	183585241	KT291500	KT291553	—	—	KT291638
<i>Caloplaca millegrana</i>	This study	Antarctica, leg. Ulrik Sochting	—	KT291502	—	KT291588	KT291640	KT291640
<i>Caloplaca ochracea</i>	GB/This study	Spain, Catalonia, Lleida prov., Spain, Catalonia, Figols i Alinyà, shadow part of Tossa de Cambrils, 1560-1620 m, 31TCG69, <i>Pinus sylvestris</i> forest, calcareous rocks and boulders, 19.9.2001, leg. P. Navarro-Rosinés (BCN).	394998688	394998519	394998583	—	KT291641	—
<i>Caloplaca polycarpa</i>	GB/This study	France, Provence, near Apt, between Rocsalère and Les Claperèdes, 500 m elev., upper part of calcareous wall, flat sun-exposed surface, facing East, 11.06.2002, leg. E. Gaya 399, C. Roux & P. Navarro-Rosinés (BCN).	183585251	KT291506	KT291556	KT291591	KT291645	KT291645
<i>Caloplaca scopularis</i>	GB	Scotland, West Ross (VC 105), Torridon, Rubha na h-Airde Glaise, and coast to north, locally abundant on rocky heavalland, grid. 18/80.56, 24.06.1994, leg. B.J. Coppins 16458, A.M. O'Dare & A.M. Fryday (E 126410).	183585266	—	—	—	394998830	—
	GB/AFToL -4820	Finland, Uusimaa, Kirkkonummi, Porkkala, Vetokannas, 59°59'N 24°25'E, on bare seashore cliffs, 20.4.2005, leg. S. Stenroos 5683 (H).	—	394998520	394998584	—	—	—
<i>Caloplaca</i> sp. 148	This study	Mexico, along road, between Ciudad Constitution and Puerto San Carlos, 25°02.337'N 111°45.814'W, 41 m, shrubs with legumes, cactuses, and <i>Fulqueria</i> , sun exposed site, flat, humid, on alive part of <i>Fulqueria</i> , leg. E. Gaya 03.04.10-12 & F. Lutzoni (DUKE).	KT291464	KT291509	KT291559	—	KT291648	—
<i>Caloplaca trachyphylla</i>	GB/This study	Pakistan (Northern Areas), NorthWestern Himalaya: rocky slopes in the gorge W, above Jutial (near Gilgit), ±1900 m, 20.07.1991, leg. J. Poelt s.n. (GZU).	183585271	KT291513	—	KT291596	KT291652	KT291652

<i>Caloplaca verruculifera</i>	GB	Iceland, INo. Eyjafjardarsysla, Silastadatangi, 65.726°N 18.143°W, ca. 1 m elev., marine habitat, 10.6.2006, leg. F. Lutzoni & C. Gueidan 06.10.07-7 (DUKE).	394998694	394998525	394998589	—	394998842	394998842
<i>Xanthomendoza borealis</i>	This study	East Antarctica, Hallett Peninsula, Cape Hallett, Ross Sea coast of Victoria Land, S 72.3167° E 170.2667°, 2006, leg. P. Crittenden (DUKE).	KT291473	KT291526	KT291567	—	KT291665	KT291665
<i>Xanthomendoza fallax</i>	GB	Alaska, 19.6.2007, leg. E. Gaya, J. Geml, J. Gomà (DUKE).	394998712	394998547	394998605	394998780	394998874	394998874
<i>Xanthomendoza mendozae</i>	GB	Bolivia, Potosí, Salar de Uyuni, Isla Inca Huasi, 20°14'39.0"S 67°37'36.1"W, 3650 m elev., on basaltic rock, leg. V. Reeb, VR 11-V-02-14 (DUKE).	394998713	394998548	394998606	—	—	394998876
<i>Xanthomendoza montana</i>	This study	USA, Arizona, Mohave County, Grand Canyon Parashant National Monument, 36°40'41"N 113°37'52"W, habitat pinyon juniper woodland, on decorticate wood <i>Ephedra</i> sp., Sandstone bluff, 20 May 2003. Collected by K.G. Sweat #KGS136A, other Collectors: S.T. Bates, B.A. Iselin & T.H. Nash III (ASU 574356).	KT291474	KT291528	KT291569	—	—	—
<i>Xanthomendoza oregana</i>	This study	USA, California, Santa Monica mountains, Rocky Oaks National Park service property, along the trail starting at the parking lot, at the 'brown house' just outside the fence around the house, 34°05.853'N 118°48.968'W, 516 m, open grassy area, sun-exposed site, dry, flat slope, on <i>Juglans californica</i> tree#4, leg. E. Gaya 03.01.10-18C & F. Lutzoni (DUKE).	—	KT291527	KT291568	KT291606	—	KT291666
<i>Xanthomendoza poeltii</i>	GB	Sweden, Halland, Övraby, Sperlingsholm, 56°42' 28.96"N 12° 53'46.93"E, 32 m elev., epiphyte on <i>Ulmus glabra</i> , 9.8.2006, leg. E. Gaya, P. Navarro-Rosinés, U. Arup, U. Sochting, N. Hladun, A. Gómez-Bolea (BCN).	394998714	394998550	394998608	394998782	394998878	394998878
<i>Xanthomendoza ulophyllodes</i>	GB	USA, Minnesota, Itasca State Park, R. Honegger 330t1 (Z+ZT).	222352298	—	—	—	—	—
	GB	Russia, 2006, leg. Urbanavichus (H; A. Thell s.n.).	—	196174856	—	—	—	—
	GB	USA, WI, Vilas co., Town of Land O'Lakes, Northern Highland State Forest, Johnson Lake Barrens State Natural Area just east of Jute Lake, NNE of Woodruff, 46°08'57"N 89°30'03"W, 545 m elev., open jack pine-aspen woods with <i>Prunus</i> and burned stumps, on dry wood, 26.4.2002, leg. R. Egan EL-15, 811 (OMA).	—	—	394998609	—	394998880	394998880
<i>Xanthomendoza weberi</i>	This study	USA, North Carolina, Wake Co., Pleasants' yard, just north of Turnipseed Preserve, rural yard facing fallow agricultural field, sunny, 35°44'52"N 78°25'16"W, ca. 73 m elevation, on trunk of large oak, 02 Apr 2011, leg. Gary B. Perlmutter #2685, det. Gary B. Perlmutter (NCU).	—	KT291529	—	KT291607	—	KT291667
<i>Xanthopeltis rupicola</i>	This study	Chile, Metropolitan Region, Cordillera Province, San José de Maipo municipality, 63km E of Santiago, following the road El Volcán, lat 33° 49' 47.3"S long 70°05'09.4"W, +/- 3 m, ca. 1759 m, saxicolous, in open well lit areas. Type locality. 10 Apr 2011 Leg R. Vargas 3638 & A. Ugarte, det R. Vargas.	—	KT291530	KT291570	KT291608	—	KT291668
<i>Xanthoria aureola</i>	GB	Sweden, Bohuslän, Kungshamn par., Sunnerskär, 58°19'42.53"N 11°14'48.12"E, 5 elev., granitic islands, 11.8.2006, leg. E. Gaya, P. Navarro-Rosinés, U. Arup, U. Sochting, N. Hladun, A. Gómez-Bolea (BCN).	394998715	394998551	394998610	394998784	394998882	394998882
<i>Xanthoria calcicola</i>	GB/This study	Spain, Catalonia, Montgrí, Cap d'Olrera, 31TEG15, on calcareous rocks, 26.5.2006, leg. X. Llimona, S. Fernández-Brime et al. (BCN).	KT291475	394998552	394998611	KT291609	394998884	394998884
<i>Xanthoria candalaria</i>	GB	France, Auvergne, Puy de Dôme, Chastreix, Puy Gros, 1793 m elev., Long E=0.530 gr. lat. 50.578 gr., Pelouses au N (cirque de la Fontaine Salée) et au sud, barre rocheuse exp. N et S., 30.8.1993, leg. X. Llimona, A. Gómez-Bolea & P. Navarro-Rosinés (BCN 8444).	183585245	—	—	—	—	—
	GB	Sweden, Halland, Varberg, Vendelsö island, 57°17'54.53"N 12° 07'29.68"E, 0-2 m elev., on siliceous rocks, 9.8.2006, leg. E. Gaya, P. Navarro-Rosinés, U. Arup, U. Sochting, N. Hladun, A. Gómez-Bolea (BCN).	—	394998553	394998612	394998786	394998886	394998886

<i>Xanthoria elegans</i>	GB	Spain, Catalonia, Lleida prov., Alt Urgell, Fígols i Alinyà, Collada de l'Estany, near Cadolla Verda, 31TCG7167, 1700- 1800 m elev., sun-lit calcareous boulders, 14.4.2000, leg. E. Gaya 192 (BCN).	183585262					
	GB	USA, Alaska, Elliott Hway, on calcareous boulder, 22.7.2007, leg. E. Gaya, J. Geml, J. Gomà (DUKE).		394998554	394998613	394998788	394998888	394998888
<i>Xanthoria parietina</i>	GB	Sweden, Bohuslän, Kungshamn par., Sunnerskär, 58°19'42.53"N 11°14'48.12"E, 5 elev., granitic islands, 11.8.2006, leg. E. Gaya, P. Navarro-Rosinés, U. Arup, U. Sochting, N. Hladun, A. Gómez-Bolea (BCN).	394998716	394998555	394998614		394998890	394998890
	GB	Switzerland, Zurich, R. Honegger 215 (Z+ZT).	222352275					—
<i>Xanthoria polycarpa</i>	GB	Sweden, Öland, Gräsgård par., E of the wall, S of the road SE Tingstenen, 56°21'05.33"N 16°28'07.07"E, 14 m elev., calcareous soils and rocks (Ordovician), 12.8.2006, leg. E. Gaya, P. Navarro-Rosinés, U. Arup, U. Sochting, N. Hladun, A. Gómez-Bolea (BCN).		394998556	394998615	394998792	394998892	—
	This study	USA, California, Santa Monica mountains, Rocky Oaks National Park service property, along the trail starting at the parking lot, at the 'brown house' just outside the fence around the house, 34°05.853'N 118°48.968'W, 516 m, open grassy area, sun-exposed site, dry, flat slope, on <i>Juglans californica</i> tree#4, leg. E. Gaya 03.01.10-18A & F. Lutzoni (DUKE).	—	KT291531	KT291571	KT291610	KT291669	KT291669

Table S4. Synopsis of alignment lengths, number of analyzed characters, number of constant and variable characters included, substitution models used for each locus, and missing sequences (absolute numbers of missing sequences and percentage of missing sequences with respect to the total number of sequences per dataset).

Locus	Alignment length	Included char.	Constant char.	Variable char.	Subst. models	Missing seq.	% Missing seq./total
5.8S	155	150	121	29 (17)	SYM + G	15	13.89%
mitSSU	940	592	417	175 (123)	HKY + I + G	7	6.48%
nucLSU	2979	1189	872	317 (188)	GTR+ I + G	22	20.37%
<i>RPB1</i> [A-D]	1146	1038	509	529 (487)	GTR+ I + G	38	35.19%
<i>RPB2</i> [5-7]	824	753	323	430 (394)	GTR+ I + G	30	27.78%
<i>RPB2</i> [7-11]	975	921	516	405 (370)	GTR+ I + G	25	23.15%
Combined data	7019	4643	2758	1885 (1579)	---	137	21.14%

Table S5. List of taxon sets included in the dating analysis of the eukaryotes dataset. Nodes that were constrained as monophyletic based on previous results (15) in the starting tree in BEAST are denoted by 'yes'. Asterisks indicate splits that were calibrated in this study.

Taxon sets	monophyly
Eudicots-Monocots*	yes
Viridiplantae	yes
Apicomplexa	yes
Stramenopiles	yes
Animalia/Choanoflagellida-Fungi*	yes
Animalia-Choanoflagellida	yes
Animalia	yes
Chordata-Urochordata*	yes
Fungi	yes
Euchytrids	yes
Blastocladiomycota*	yes
Zygomycota	yes
Glomeromycota-Mucormycotina*	no
Mucormycotina	yes
Glomeromycota	yes
Basidiomycetes-Ascomycetes	yes
Basidiomycetes	yes
Pucciniomycotina	yes
Ustilaginomycotina	yes
Agaricomycotina	yes
Marasmiaceae-Pleurotaceae*	no
Mycenaceae-Agaricaceae*	no
Ascomycetes	yes
Saccharomycotina	yes
Pezizomycotina	yes
Orbiliomycetes	yes
Pezizomycetes-Leotiomyceta*	no
Pezizomycetes	yes
Leotiomyceta	yes
Dothideomycetes-Arthoniomycetes*	no
Sordariomycetes	yes
Leotiomycetes	yes
Eurotiomycetes	yes
Eurotiales-Onygenales	yes
Pyrenulales	yes
Verrucariales	yes
Chaetothyriomycetidae	yes
Chaetothyriales	yes
Lecanoromycetes	yes
<i>Anzia-Canoparmelia*</i>	yes
Teloschistales	yes
Peltigerales	yes

Table S6. List of the ten calibrations used in this study (eukaryotes dataset) following (15) with a few modifications. For fossil data we included information on their age, locality and publication. For each calibration, the parameters used to set the priors are provided.

Node	Species	Calibration	Date (myr)	Geological period	Locality	Publication*	Calibration prior		
							Mean	Log(stdev)	Offset
Basal fungal lineages									
1	Arbuscular mycorrhizal fungi	Split Glomeromycota-Mucormycotina	460	Ordovician	Wisconsin	Redecker <i>et al.</i> 2000 (22)	460 ^a	0.2	90
2	<i>Allomyces</i>	Split <i>Allomyces-Physoderma</i>	400	Devonian	Scotland	Taylor <i>et al.</i> 1994 (23)	400 ^a	0.2	5
Basidiomycetes									
3	<i>Archaeomarasmius leggetti</i>	Split Marasmiaceae-Pleurotaceae	90-94	mid Cretaceous	New Jersey	Hibbett <i>et al.</i> 1997 (24)	92 ^a	0.2	45
4	<i>Protomyces electra</i>	Split Mycenaceae-Agaricaceae	15-20	Miocene	Dominican Rep.	Hibbett <i>et al.</i> 1997 (24)	17.5 ^a	0.2	10
Ascomycetes									
5	<i>Palaeopyrenomycites devonicus</i>	Split Pezizomycetes-Leotiomyceta	400	lower Devonian	Scotland	Taylor <i>et al.</i> 1999 (25)	400 ^a	0.2	160
6	<i>Anzia electra</i>	Split <i>Anzia-Canoparmelia</i>	40	Tertiary, Eocene	Baltic	Rikkinen & Poinar 2002 (26)	40 ^a	0.2	30
7	Sooty molds and <i>Curvularia</i> -type spores	Split Dothideomycetes-Arthoniomycetes	93-95	mid Cenomanian	Ethiopia	Schmidt <i>et al.</i> 2010 (27)	94 ^a	0.2	72
Plants									
8	Appearance of tricolpate pollen	Split Eudicots-Monocots	125	early Cretaceous	Worldwide	Crane <i>et al.</i> 1995 (28)	125 ^b	0.2	-
Secondary calibrations									
9	Split Urochordata-Chordata	Molecular-based calibration	600 (565-643)	Precambrian	-	Douzery <i>et al.</i> 2004 (29)	600 ^b	0.2	-
10	Split Fungi-Animalia/Choanoflagellida	Molecular-based calibration	983 (872-1127)	Precambrian	-	Douzery <i>et al.</i> 2004 (29)	983 ^a	0.0715	15

a For priors using a log normal distribution, the mean, the log(standard deviation) and the value of the offset are provided.

b For priors using a normal distribution, only the mean and the log(standard deviation) are given.

* For references, please see supplementary references list (above).

Table S7. List of nine calibrated nodes obtained from the first-step dating analysis (Fig. S6; eukaryotes dataset) and used as constraints in the dating analysis of the Teloschistales dataset (Fig. S1).

Node	Calibration	Calibration prior	
		Mean (Mya)	Log(stdev)
A	Split Megalosporaceae and Teloschistaceae	148.7	16
B	Split <i>Megalospora</i> - <i>Megaloblastenia</i>	75.1	18
C	Split <i>Brigantiaea leucoxantha</i> - <i>B. tricolor</i>	10.6	3.7
D	Split <i>Letrouitia domingensis</i> - <i>L. vulpina</i>	13.9	4.5
E	Split Brigantiaeaceae-Letrouitiaceae	94.5	20
F	Split <i>Caloplaca</i> - <i>Huea</i>	59.3	14.5
G	Split <i>Caloplaca</i> - <i>Huea</i> and <i>Ioplaca</i>	88.1	14
H	Split <i>Caloplaca</i> - <i>Xanthoria</i>	43.5	8.4
I	Split <i>Caloplaca</i> - <i>Xanthoria</i> and <i>Xanthomendoza</i>	72.5	11.5

Table S8. Divergence time estimates for the main splits in the Teloschistales. For each divergence, the mean and the 95% confidence interval are reported. The results are provided in millions of years (Mya). The node numbers provided in this table were also used in Fig. S1 to show their placement in the chronogram.

Node	Age	95% confidence interval
1	162.22	193.19 - 132.84
2	144.63	167.72 - 122.56
3	98.48	113.47 - 82.73
4	90.21	104.86 - 75.53
5	85.65	99.43 - 71.82
6	83.25	104.25 - 63.29
7	81.00	102.95 - 60.80
8	71.91	85.00 - 58.51
9	65.31	82.78 - 47.87
10	62.61	74.03 - 51.85
11	57.33	67.53 - 47.11
12	50.63	68.82 - 33.65
13	43.01	50.01 - 36.11
14	16.53	21.40 - 11.84

Table S9. Harmonic means and Bayes Factors from comparison between best models in BayesTraits analyses for the different traits examined. Comparisons were between Reversible Jump Hyper Prior (RJHP), and unconstrained model without RJHP, and a constrained model with equal rates ($q_{AB}=q_{BA}$).

BayesTraits	ANTHRA THALLUS	ANTHRAQUINONES	SHADE	ROCK	BARK	CRUST. CONTINUOUS	ATTACH. STRUCTURES
RJHP analyses							
	Harmonic mean						
hpall="exp 0 0.1", rjhp="exp 0 0.1"	-31.57859	-17.52897	-53.964481	-59.09209	-62.57761	-63.86969	-41.54682
hpall="exp 0 1", rjhp="exp 0 1"	-31.51565	-17.40939	-55.349016	-57.03865	-63.0575	-66.21248	-41.61517
hpall="exp 0 10", rjhp="exp 0 10"	-31.41062	-17.61419	-54.00728	-60.11743	-64.177	-65.17292	-41.63654
hpall="exp 0 100", rjhp="exp 0 100"	-31.45092	-31.33212	-55.005814	-57.82174	-65.38471	-67.06816	-41.56381
hpall="exp 0 0.01", rjhp="exp 0 0.01"	-62.52974	-31.26221	-57.87086	-67.61668	-62.66752	-62.85751	-51.00922
Unconstrained analyses							
	Harmonic mean						
hpall="exp 0 0.1"	-33.82467	-18.28087	-54.30109	-57.91602	-64.0783	-63.05631	-39.74294
hpall="exp 0 1"	-32.66864	-19.19641	-56.655326	-61.65305	-66.6843	-64.82426	-40.67598
hpall="exp 0 10"	-32.49832	-20.19122	-58.266982	-66.70843	-70.89303	-65.82882	-46.0865
hpall="exp 0 100"	-62.49694	-31.33216	-58.193431	-67.79769	-70.94169	-73.08366	-44.12625
hpall="exp 0 0.01"	-63.089	-31.62883	-57.749151	-68.01018	-71.07046	-74.14817	-51.97639
Constrained $q_{AB}=q_{BA}$ analyses							
	Harmonic mean						
hpall="exp 0 0.1"	-31.17908	-17.66699	-52.95457	-56.6563	-63.654	-63.37114	-41.64833
hpall="exp 0 1"	-31.34681	-18.13877	-57.83131	-56.86561	-66.78067	-67.33973	-41.4634
hpall="exp 0 10"	-31.34779	-17.33716	-54.17114	-57.42203	-67.91257	-66.76336	-41.43208
hpall="exp 0 100"	-31.54685	-17.73291	-59.05591	-57.23471	-65.08637	-66.26756	-41.31742
hpall="exp 0 0.01"	-31.61472	-17.93936	-52.84167	-56.85294	-62.62203	-62.83	-40.83503
BF Comparisons Between Best Analyses							
	bf.test($q_{AB}=q_{BA}$ *, Unconstrained*)	bf.test($q_{AB}=q_{BA}$ *, Unconstrained*)	bf.test($q_{AB}=q_{BA}$ *, Unconstrained*)	bf.test($q_{AB}=q_{BA}$ *, Unconstrained*)	bf.test($q_{AB}=q_{BA}$ *, Unconstrained*)	bf.test($q_{AB}=q_{BA}$ *, Unconstrained*)	bf.test($q_{AB}=q_{BA}$ *, Unconstrained*)
	BF BestModel	BF BestModel	BF BestModel	BF BestModel	BF BestModel	BF BestModel	BF BestModel
	2.638482 Model 1	1.887412 Model 1	2.91884 Model 1	2.51944 Model 1	2.91253 Model 1	0.45261 Model 1	2.184176 Model 2
	bf.test($q_{AB}=q_{BA}$ *, RJHP*)	bf.test($q_{AB}=q_{BA}$ *, RJHP*)	bf.test($q_{AB}=q_{BA}$ *, RJHP*)	bf.test($q_{AB}=q_{BA}$ *, RJHP*)	bf.test($q_{AB}=q_{BA}$ *, RJHP*)	bf.test($q_{AB}=q_{BA}$ *, RJHP*)	bf.test(RJHP*, Unconstrained*)
	BF BestModel	BF BestModel	BF BestModel	BF BestModel	BF BestModel	BF BestModel	BF BestModel
	0.463072 Model 1	0.144462 Model 1	2.245622 Model 1	0.7647 Model 1	0.088846 Model 2	0.055006 Model 1	3.607764 Model 2

Table S10. Summary of log likelihood and AICs of the *corHMM* analyses considering different initial values used for the likelihood search (ip) and rate categories.

<i>corHMM</i>	rate.cat=1			rate.cat=2			Δ AICc
	-lnL	AIC	AICc	-lnL	AIC	AICc	
Anthra. Thallus							
ip=0.01	-30.87712	65.75423	65.86852	-29.49696	74.99393	76.44847	-10.57995
ip=0.1	-30.87719	65.75438	65.86867	-29.64128	75.28256	76.7371	-10.86843
ip=1	-62.2987	128.5974	128.7117	-59.23201	134.464	135.9186	-7.2069
Anthraquinones							
ip=0.01	-16.84495	37.6899	37.80418	-14.35183	44.70366	46.15821	-8.35403
ip=0.1	-16.84463	37.68926	37.80355	-15.42961	46.85921	48.31376	-10.51021
ip=1	-16.84502	37.69003	37.80432	-15.45154	46.90308	48.35763	-10.55331
Shade							
ip=0.01	-53.29916	110.5983	110.7126	-44.95643	105.9129	107.3674	3.3452
ip=0.1	-53.29937	110.5987	110.713	-50.07407	116.1481	117.6027	-6.8897
ip=1	-57.25084	118.5017	118.616	-56.3503	128.7006	130.1551	-11.5391
Rock substrate							
ip=0.01	-56.68839	117.3768	117.4911	-53.5715	123.143	124.5975	-7.1064
ip=0.1	-56.68799	117.376	117.4903	-50.55073	117.1015	118.556	-1.0657
ip=1	-67.36646	138.7329	138.8472	-66.59407	149.1881	150.6427	-11.7955
Bark							
ip=0.01	-62.45666	128.9133	129.0276	-57.73942	131.4788	132.9334	-3.9058
ip=0.1	-62.45838	128.9168	129.031	-59.14204	134.2841	135.7386	-6.7076
ip=1	-70.63774	145.2755	145.3898	-61.38762	140.2298	140.2298	5.16
Crust. continuous							
ip=0.01	-61.06412	126.1282	126.2425	-59.04375	134.0875	135.542	-9.2995
ip=0.1	-61.06464	126.1293	126.2436	-57.12944	130.2589	131.7134	-5.4698
ip=1	-61.06413	126.1283	126.2425	-71.94724	159.8945	161.349	-35.1065
Attach. Structure							
ip=0.01	-38.33191	80.66382	80.77811	-37.23463	90.46926	91.9238	-11.14569
ip=0.1	-38.33178	80.66357	80.77785	-36.73539	89.47078	90.92532	-10.14747
ip=1	-38.33166	80.66332	80.7776	-49.41205	114.8241	116.2786	-35.501

Note: In all analyses node.states="marginal", n.cores=8, root.p="maddfitz", and compared with nstarts=100